Breitfeld H. Tim (Orcid ID: 0000-0002-9563-1862)

Origin of Lower Cretaceous quartzose arenites in northern India and the Indus Basins of Pakistan – the result of provenance composition, weathering or diagenesis?

Hazel Beaumont[1]*, Stuart D. Burley[2&3], Tim Breitfeld[4], Thomas Gould[5] and Stuart M. Clarke[2]

[1] Department of Geography and Environmental Management, University of the West of England, Bristol, UK
* hazel.beaumont@uwe.ac.uk
[2] Basin Dynamics Research Group, Keele University, Keele, Staffordshire, UK
[3] Discovery Geoscience, Lapworth Croft Lodge, Warwickshire, UK
[4] Department of Exogene Geologie & Sedimentologie, TU Bergakademie Freiberg, D-09599, Germany
[5] PetroStrat, Century House, Gadbrook Business Centre, Northwich, UK

Abstract

Lower Cretaceous (Aptian-Albian) sandstones of the Ghaggar-Hakra Formation in the Barmer Basin of northwest Rajasthan, India, have a complex depositional history which is confusing given they are quartzose arenites. The heavy mineral grains are very well-rounded and the assemblage is dominated by zircon and rutile grains suggesting that the sediments have been recycled multiple times, whilst the presence of staurolite indicates a metapelite provenance component. Petrographical analysis suggests that extreme diagenesis cannot account for the quartzose arenite composition, despite Early Cretaceous soil formation and at least two periods of subsequent telogenetic modification. An alternative explanation to extreme chemical weathering in the provenance area is that the Ghaggar-Hakra sandstones are multi-cycle sediments derived, at least in part, from the quartzose arenites of the Cambrian Jodhpur Group.

This analysis suggest that variations in detrital mineralogy across the Western India Rift System and Indus Basins are the result of transcontinental fluvial transport systems sourcing sediment from specific basement highs (Nagar Parker High, Devikot High, Deodar Ridge and Aravalli Mountain Range) mixed with varying proportions of sediment derived from sandstones of the Jodhpur Group. Consequently, we suggest that Cretaceous fluvial systems were controlled by the local palaeogeographies within the failed rifts of the Barmer and Cambay Basins, and that both basins formed barriers to sediment transport from the Aravalli Mountain Range across the north-west Indian plate and into surrounding basins.

Acknowledgements

This research was undertaken with matched funding from the Keele University Acorn Fund and Caim India Limited. The heavy mineral separation would not have been possible without support from the Daniel Pidgeon Fund of the Geological Society of London which is gratefully acknowledged. Cairn India Limited generously provided logistical support for all fieldwork in Rajasthan where Bhanwar Lal, Andrew Bladon and James Solan are also thanked for their practical assistance and good humour in the field. LST laboratory work was undertaken at University of the West of England with huge thanks to Andrew Geary for all his support. Juliane Hennig-Breitfeld and Tim Pearce are thanked for Raman Spectroscopic analysis of heavy minerals at Chemostrat Ltd. Conceptualisation of this work was by SMC & SDB; Analytical work was completed by HB, SDB, TB, TG; Interpretation HB, SDB, TB; Writing HB, SDB, and Edits: SMC.

Introduction

Provenance is a well-established primary control on the detrital and authigenic mineralogy of sandstones which can be influenced by weathering in the source and depositional areas (Suttner *et al*., 1981; Johnsson *et al.,* 1988). Tropical weathering in deep soil profiles can remove all labile minerals leaving only a quartz framework for transport, resulting in quartzose arenites as the sedimentary product (Dutta, 1992; Anand, 2002). Moreover, the effects of *in-situ* diagenesis can remove feldspars, ferro-magnesium minerals and heavy minerals from the sedimentary record (Garzanti, 2017). To fully unravel provenance and to relate sandstone mineralogy to potential provenance areas, the original mineralogy must be reconstructed by adjusting the current mineralogy to allow for the effects of *in-situ* weathering and diagenesis which is undertaken here based on the observed diagenetic effects. To reconstruct original provenance more accurately, the original proportions feldspar, ferromagnesium mineral grains, and unstable lithic fragments prior to weathering need to be estimated.

Lower Cretaceous sandstones on the northwest Indian Plate are preserved in widely scattered outcrops within inverted rift basins, where they have been at least partially protected from the erosional effects of end-Cretaceous and Oligocene uplift events (Biswas, 1999; Racey *et al*., 2016; Najman *et al*., 2018). The sediments were deposited by large-scale fluvial to shallow marine systems (Figure 1) within the developing West Indian Rift System (WIRS) that comprises the Barmer, Camby, Kachchh and Narmada basins. Despite the wide range of basement lithologies exposed in the Cretaceous Period, many of these sandstones are mineralogically quartzose arenites (Akhtar & Ahmad, 1991; Racey, et al., 2016; Rajak et al., 2022). In Pakistan, time-equivalent strata of the WIRS are the Goru and Sembar formation of the Lower and Middle Indus basins (LMIBs; Figures 1 & 2). Sediments of both these formations include quartzose arenites (Baig *et al.,* 2016; Ismail *et al.,* 2018). It is generally assumed that the provenance for many of the Lower Cretaceous depositional systems is the Aravalli Mountain Range as this is likely to have been upland terrain in the Cretaceous Period (Biswas, 1999; Chaudhuri *et al*., 2020a; c.f. Racey *et al*., 2016; Rajak *et al.,* 2022).

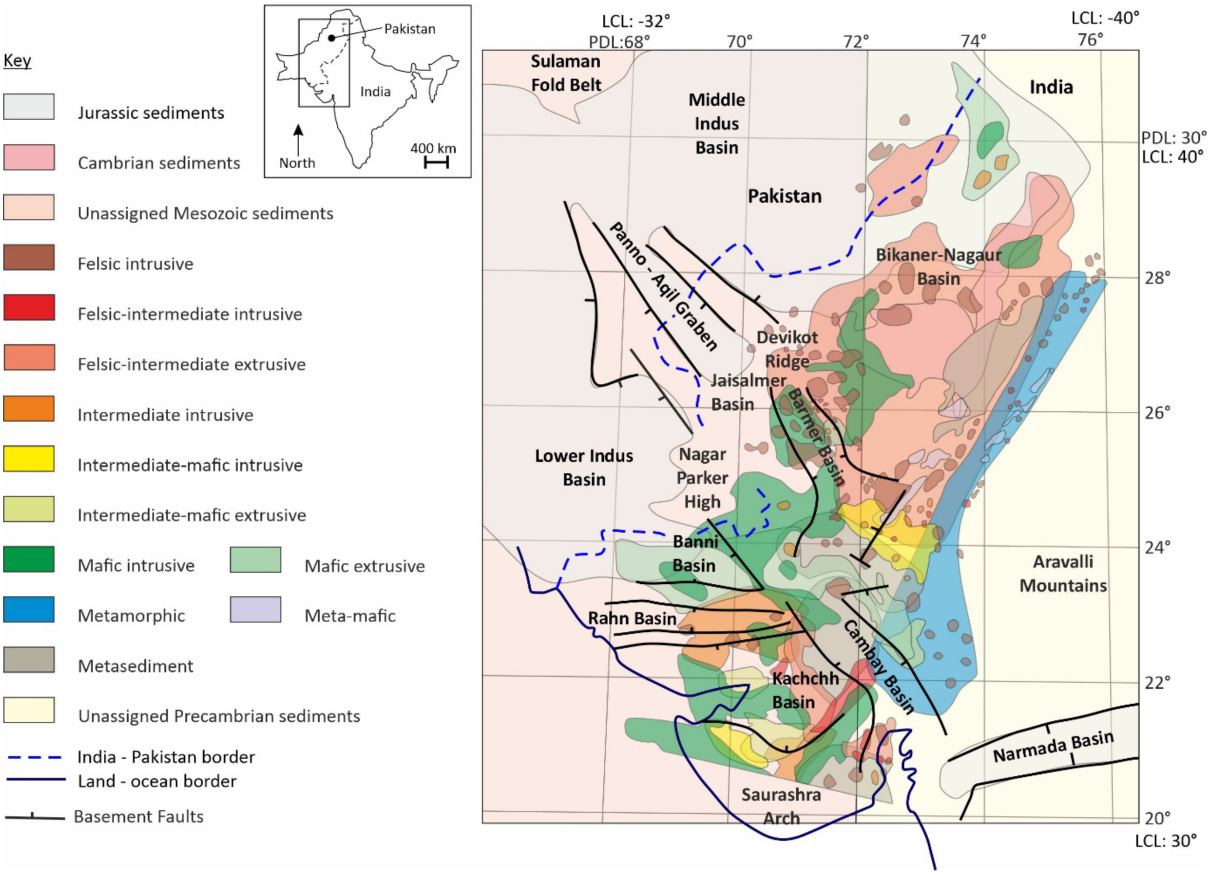

Figure 1: Location of the WIRS and the LMIB (adapted from Balakrishnan *et al.,* 2009) on the northern Indian Plate with various locations named that are in the text, overlain on a reconstruction of the pre-Cretaceous basement geology (Roy and Jokhar, 2002; Kothari *et al.,* 2015; Dolson *et al.,* 2015). The WIRS and LMIBs meet at the country borders. Extrapolation of basement geology to sub-crop areas is based on published gravity and magnetic maps using the following rules-of-thumb (i) very dense and highly magnetic bodies are interpreted to be mafic intrusions. (ii) local circular to elliptic lows in the gravity data are interpreted to be felsic to intermediate intrusive bodies; and (iii) metasediments are mapped in areas of mostly low gravity signal and weak magnetic response.

In this paper we present new textural and mineralogical petrographical data for sandstones of the Lower Cretaceous Ghaggar-Hakra Formation of the Barmer Basin that are exposed at Sarnoo, 40 km east-southeast of Barmer on the eastern rift margin. For comparison, we compile previously published detrital mineralogical data from Lower Cretaceous sandstones across the WIRS and LMIB. We review the provenance terrains of the Lower Cretaceous sandstones in the light of detailed palaeogeographical reconstructions as set out by Beaumont *et al*. (2019) to constrain in detail the spatial and temporal patterns of sediment dispersal systems.

Geological context

Northwestern India and eastern Pakistan together formed the northern leading margin of the Indian Plate during its break-away from Gondwana in the Late Triassic Period. These two areas have a complex Mesozoic geological history (Biswas, 1999**;** Torsvik *et al*., 2000; Chatterjee *et al*., 2013) which is preserved in small, scattered outcrops across the northern Indian Plate (Akhtar & Ahmad, 1991; Casshyap & Aslam 1992; Akhtar *et al*., 1996; Bhatt *et al*., 2016; Beaumont *et al*., 2019). A more complete Mesozoic succession is reported in the subsurface of the Barmer Basin, as recorded from well and seismic data (Dolson *et al*., 2015; Kothari *et al.,* 2015), and in the subsurface of LMIB (Ahmad & Chaudhry, 2002; Berger *et al*., 2009; Baig *et al*., 2016).

The geological evolution of the WIRS and LMIB comprises four major tectonic events:

1) Late Triassic to Early Jurassic break-up of eastern Gondwana (Biswas, 1999, 2005; Wandrey *et al*., 2004) which reactivated faulting along the Aravalli-Delhi Mountain Range to form deep rifts within the present-day locations of the Kachchh and Indus basins;

2) The initial separation of Madagascar from the Indian Plate (120 Ma, Marks & Tikku, 2001; Biswas, 2005) led to the initial development of the Cambay, Barmer and Narmada basins of the WIRS, along with deepening of the Kachchh and Indus basins. As India moved northwards and rotated counter-clockwise (88 – 84 Ma, Wandrey *et al*., 2004; Collier *et al*., 2008) subsidence, accompanied by sedimentation, occurred throughout the northern Indian Plate with opening of the Indian Ocean due to the separation of India from Africa in the late Cretaceous Period.

3) Close to the time of Cretaceous – Palaeogene boundary, the Seychelles micro-continent separated from western India. The separation coincided with, and may be related to, the eruption of the Deccan Traps and the passage of the proto-Reunion hot spot. These events are associated with widespread uplift of the northwest margin of the Indian Plate that forced general eastward-draining fluvial systems to re-orientate to the west (Cox, 1989; Gombos *et al*., 1995; Sheth, 2007) and caused regional planation surfaces (Sheth, 2007), and;

4) The Cenozoic Era was characterised by fault-controlled deepening and infilling of the Barmer and Cambay basins with more than 6 km of sediments deposited in continental settings (Sisodia & Singh, 2000; Roy & Jokhar, 2002; Tabaei & Singh, 2002; Tripath *et al*., 2009;

Dolson *et al*., 2015). During the Oligocene Epoch, the continued collision of the Indian Plate with the Eurasian Plate caused uplift and erosion (Compton, 2009; Chatterjee *et al*., 2013; Dolson *et al*., 2015; Najman *et al*., 2018).

Basement terrains in north-western India

The basement rocks of the north-western Indian Plate comprise the Malani Igneous Suite (age: 745+/-10 Ma, Bushan, 2000), Saurasthra Arch, the Nagar Parkar Igneous Suite exposed in the Nagar Parkar High, the Banded Gneissic Complex, the rocks of the Devikot Ridge and the northwest – southeast oriented, eroded remnants of the Precambrian Aravalli Mountain Range (including the Aravalli, Bhilwara, Delhi and Marwar supergroups, Erinpura and Idar granites,~2000 Ma, Goodwin, 1991; McKenzie *et al.,* 2013). The Bundelkhand Gneissic Craton, east of the Aravalli Mountain range, is a potential basement source terrain, which comprises the Bundelkhand massif, Bijawar and Gwalior Group of rocks and late Precambrian Vindhyan sediments (Sharma, 2000; Rao et al., 2005; Bhattacharya and Singh, 2013; Singh and Divedi, 2015). These areas are the main provenance terrains for all sediments on the northern margin of the Indian Plate (Figure 1). The basement composition of the Pachham High Jacobad High and Kandkot Highs in eastern Pakistan are poorly known.

Potential provenance locations

The Malani Igneous Suite contains several types of extrusive volcanic materials, including A-type porphyritic rhyolite displaying a granophyric texture with volcanic flow textures and containing quartz, sanidine, perthite, hornblende, muscovite, zircon and opaques; non-porphyritic rhyolite (Bhushan, 1985; Singh *et al*., 2006) with microcrystalline and glomeroporphyritic textures containing quartz, alkali feldspar (sanidine, perthite), alkali amphibole (arfvedsonite, riebeckite), aegirine, zircon and opaques; trachyte displaying porphyritic and microcrystalline textures and contains alkali feldspar, alkali amphibole, quartz, zircon and opaques (Bhushan, 1985; Singh *et al*., 2006); and intrusive hypabyssal volcanics (Bhushan, 1985).

Directly overlying the Malani Igneous Suite are strata of the Neoproterozoic to Cambrian Marwar Supergroup. These comprise unmetamorphosed and undeformed fluvial and marginal marine siliciclastics, marine carbonates and minor volcaniclastics (George & Ray, 2017). Although covered extensively by Quaternary deposits, isolated outcrops, seismic data and well penetrations indicate that strata the Marwar Supergroup onlap onto the rocks of the Malani Igneous Suite to the south, and likely covered a large area of north-western India before the Cretaceous. They are bound to the east by the Aravalli Mountain Range. To the north and west the sediments of the Marwar Supergroup are on-lapped by Palaeozoic (Pandey *et al.,* 2009) and Mesozoic sediments (Davies *et al*., 2014).

The siliciclastic sediments of the Marwar Supergroup are quartzose arenites (Kumar *et al*., 2011) of the Sonia, Girbhakar, Nagaur and Tunklian sandstones that together comprise the Jodhpur Group. These were sourced primarily from the sediments of the Malani Igneous Suite, the faulted and folded supracrustal rocks of the Delhi Supergroup (Biju-Sekhar *et al.,* 2003) with sediments deposited in fluvial and shallow marine coastal zones (Singh, 1988; Chauhan and Ram, 1999). Another potential source of the Marwar Supergroup are the Banded Gneiss Complexes (George & Ray, 2017) comprising amphibole to granulite grade tonalitic gneisses, metabasic rocks, migmatites and schists (Heron, 1953; George & Ray, 2017). The geochemistry of quartzose arenites of the Marwar Supergroup does not indicate any sediment supply from the Malani Igneous Suite, except for those deposited directly on top of the Malani Igneous Suite (George & Ray, 2017). There are few petrographic descriptions of the Marwar Supergroup, so the diagenetic mineralogy and abundance of quartz overgrowths in these sequences is not known in detail. Kumar *et al*. (2011) document the presence of small quartz overgrowths in concretions in the Sonia Sandstone.

Within the WIRS, the time-equivalents of the Marwar Supergroup comprise the Lower Cambrian Birmania and Randha formations. The Birmania Formation contains three marine successions (Mahashwari *et al*., 2007), while the Randha Formation comprises mudstone interbedded with thick, cross-bedded sandstone units (Sisodia & Singh, 2000) that were deposited within a littoral setting (Mahashwari *et al*., 2000). Across the northwest margin of the Indian Plate the interbedded fluvial to shallow marine sandstones and siltstones of the Permian Bhuana Formation rest with marked unconformity on older rocks (Zadan & Arbab, 2015). The Jurassic Lathi Formation comprise a thick succession of dominantly medium-grained, trough cross-bedded sandstones, with abundant fossilised wood remains, deposited within a braided fluvial system (Pandey *et al.,* 2012). Lathi Formation sandstones are quartz arenites with <3% feldspar (Ahmad *et al*., 2000), considered to be sourced from the Aravalli-Delhi fold belt, although polycyclic. They are devoid of quartz overgrowths (Alam *et al*., 2000).

Lower Cretaceous sediments of the Indian Plate

The Lower Cretaceous sediments within the north-western Indian Plate were deposited within continental to shallow marine environments (Akhtar & Ahmad, 1991; Mohan, 1995; Kundal & Sanganwar, 1998; Singh, 2006; Mude *et al*., 2012; Naseer *et al*., 2014; Racey *et al*., 2016; Beaumont *et al*., 2019, their Figure 12). Fluvial sediments of Lower Cretaceous age are present within the Barmer, Narmada, Cambay and Jaisalmer basins; sediments of equivalent age, but of a dominantly shallow marine origin, are preserved in the Kachchh Basin and in the LMIB (Figure 2; Table 1).

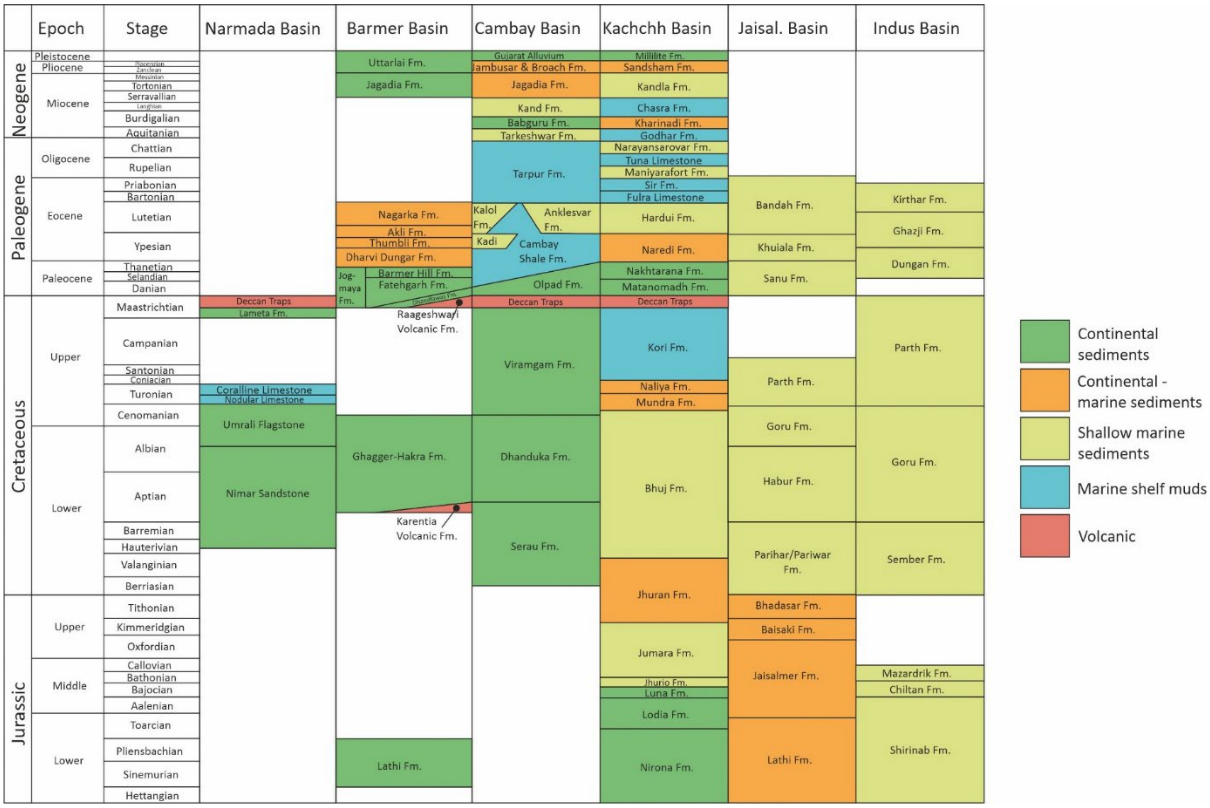

Figure 2: Summary stratigraphy for the basins of the Indian Plate, compiled from Srivastava *et al.*, (1980); Mukherjee (1983), Biswas (1987) Desai & Desai (1989), Racey *et al.* (2016); Krishna 1987; Singh, 2006; Afzal *et al.*, 2009).

Formation	Basin	Texture	Composition	Palaeoflow
Nimar Sandstone	Narmada Basin	Sub-angular to sub-rounded coarse-grained sandstones (Akhtar & Ahmad,	Monocrystalline quartz, subordinate rock fragments of metamorphic and sedimentary origins (Akhtar & Ahmad, 1991; Racey *et al*., 2016), with detrital	To the southwest – west (Ahmad &

		1991; Kundal & Sanganwar, 1998)	micas, rounded feldspar and rounded heavy minerals	Akhtar, 1990)
Himatnagar Sandstone	Cambay Basin	Moderately sorted, sub-angular fine- to coarse-grained sandstones, with textural immaturity (Desai & Desai, 1989).	95% detrital quartz grains, subordinate feldspars and minor heavy minerals (Desai & Desai, 1989).	To the west (Desai & Desai, 1989)
Bhuj Formation	Kachchh Basin	Well sorted (Bose *et al.*, 1986), sub-angular to sub-rounded grains (Chardhuri *et al.*, 2020a).	Monocrystalline quartz grains with low-grade metamorphic fragments and moderate amounts of K-feldspar (Racey *et al.*, 2016; Chardhuri *et al.*, 2020c).	To the southwest (Mandal *et al.*, 2016).
Goru and Sembar sandstones	Indus Basin	Medium- to coarse-grained	Dominated by monocrystalline and polycrystalline quartz and feldspar detrital minerals with carbonate fragments, muscovite and biotite; also, tourmaline and zircon heavy minerals (Berger *et al.*, 2009). Authigenic cements include quartz, chlorite and carbonate cements with a porosity ranging from 2 to 22% (Berger *et al.*, 2009).	To the west (Ahmad *et al.*, 2004)

Table 1: Summary of textural, compositional and palaeoflow data for Lower Cretaceous Sandstones from the WIRS and LMIB; references are within the table.

<u>The Ghaggar-Hakra Formation of the Barmer Basin</u>

Strata of the Lower Cretaceous Ghaggar-Hakra Formation occur unconformably over the Malani Igneous Suite in the Barmer Basin. The Ghaggar-Hakra Formation represents an intra-continental fluvial deposit and comprises three distinct sandstone units, together with floodplain mudstones and associated stabilised palaeosols (Beaumont *et al.*, 2019). The oldest sandstone unit, the Darjaniyon-ki Dhani Sandstone (Figures 3 & 4**;** Bladon *et al.*, 2015), was deposited as transient gravel bars, isolated channels and ephemeral floodplain deposits representing a bed load-dominant, highly avulsive, low sinuosity, fluvial system. The overlying Sarnoo Sandstone (Figures 3 & 4) is a fine- to coarse-grained, generally well sorted sandstone succession comprising laterally and vertically stacked sediments deposited within channels and their associated point bars, indicating deposition in a mixed load, highly sinuous fluvial system. Capping the Ghaggar-Hakra Formation at outcrop is the Nosar Sandstone (Figures 3 & 4), a coarse-grained fluvial unit with an erosional sixth-order basal bounding surface. The Nosar Sandstone comprises stacked and amalgamated channel and gravel bar sediments, with small, isolated packages of floodplain sediments. It illustrates the deposits of a bedload dominant, low sinuosity fluvial system.

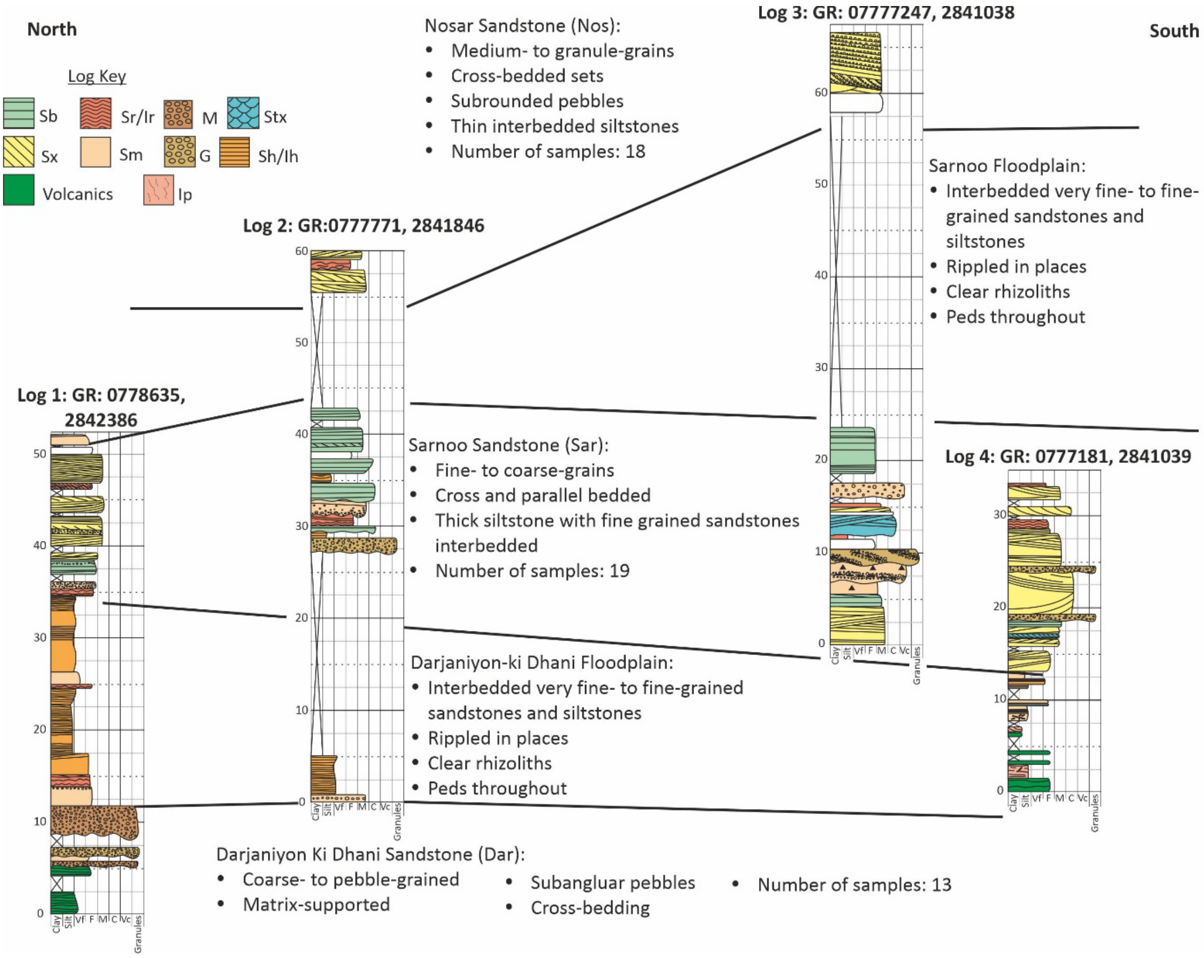

Figure 3: Sedimentological log correlation panel displaying the vertical and lateral facies variation of the Ghaggar-Hakra Formation sequence; GR – Grid Reference in UTM, Zone 42 R. Key: Sb – Parallel-bedded Sandstone, Sr – Rippled Sandstone, Ir – Rippled Siltstone, M – Matrix-supported conglomerate, Stx – Trough Cross-bedded Sandstone, Sx – Planar Cross-bedded Sandstone, Sm – Massive Sandstone, G – Clast-supported Conglomerate, Sh – Horizontally-laminated Sandstone, Ih – Horizontally-laminated Siltstone, Ip – Pedogenic Siltstone.

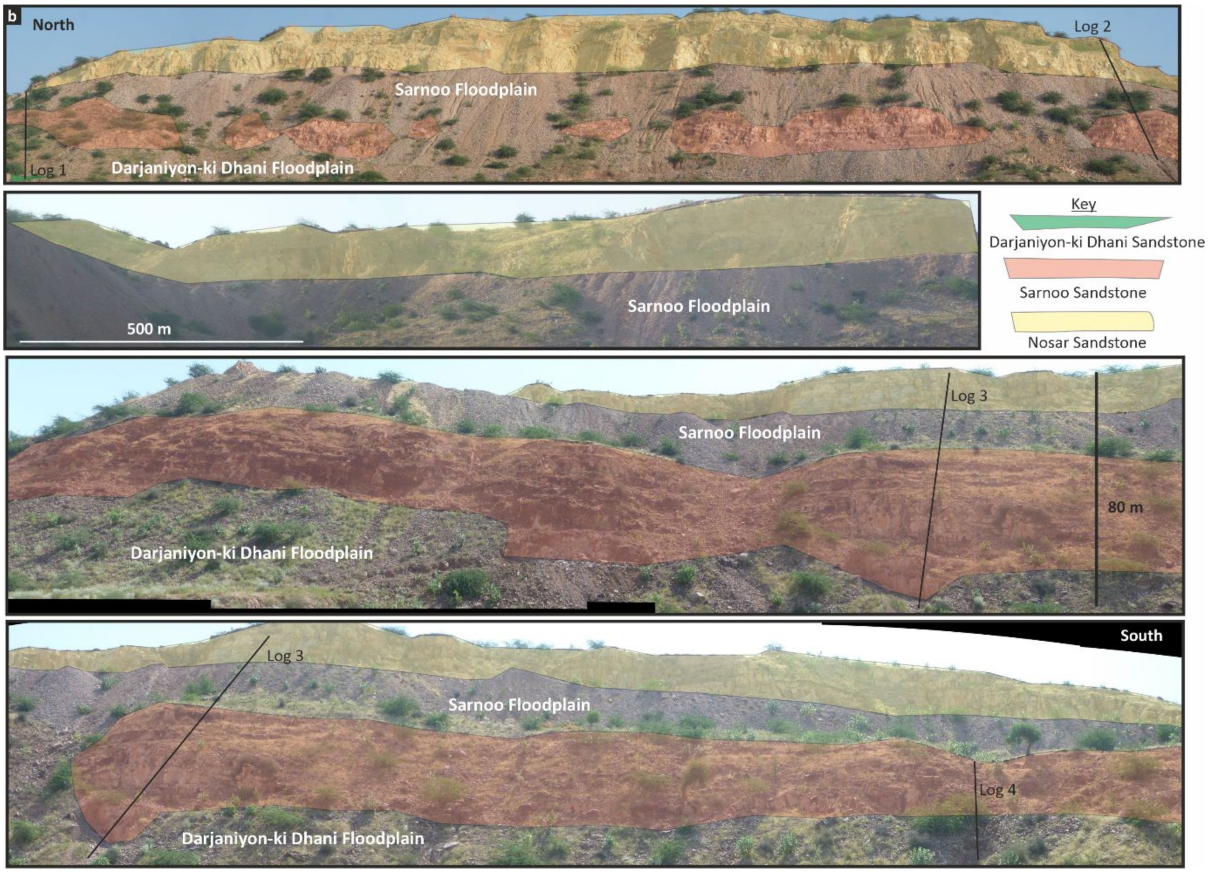

Figure 4: Photograph montage panels covering the log correlation panel in Figure 3 (log locations marked) displaying the thickness of the distinct packages; the sections without a colour overlay are covered in scree and are interpreted to be mudstones with palaeosols.

The successions preserved between sandstone units comprise pedogenically modified fine-grained sandstones and siltstones deposited in floodplain settings. Each succession is named after the sandstone it succeeds (Figure 4). From the base of the Darjaniyon-ki Dhani Sandstone to the top Sarnoo Floodplain succession, the sediments indicate a morphing of the fluvial style from low to high sinuosity with time that is typical of most fluvial systems (Schumm, 1981). The base of the Nosar Sandstone is highly erosive and the increase in sediment transported and deposited by bedload and within transient bars is indicative of rejuvenation of the fluvial system (Beaumont *et al*., 2019).

Preserved soil profiles reach up to 40 m in thickness in sediments of the Darjaniyon-ki Dhani Floodplain (Figures 3, 4 & 5) and are colour-mottled from purplish red through orange to pale greenish-blue, with the pale colours typically representing iron oxidation-reduction reactions associated with organic material. A pronounced pedogenic fabric associated with rootlets is present in the upper part of this profile, with concentric colour mottling around the rootlets, and local rhizolith concretions (Figure 5; Beaumont *et al*., 2019). Small calcite and siderite nodules are present in the upper part of the floodplain sediments, but the siderite is highly oxidized to a suite of iron oxides, most likely due to soil-forming redoximorphic (oxidation-reduction) reactions (Driese *et al*., 1995; Salama & Anand, 2017). The floodplain succession also includes highly rippled and cross-laminated fine-grained sandstones and siltstones representing deposition in small ephemeral ponds. Within the sediments of the Sarnoo floodplain, rhizoliths are absent and the rippled sections are fewer compared to the lower floodplain sections, although the colour mottling and calcrete nodules are more frequent. These features probably indicate a more established floodplain (Beaumont *et al*., 2019).

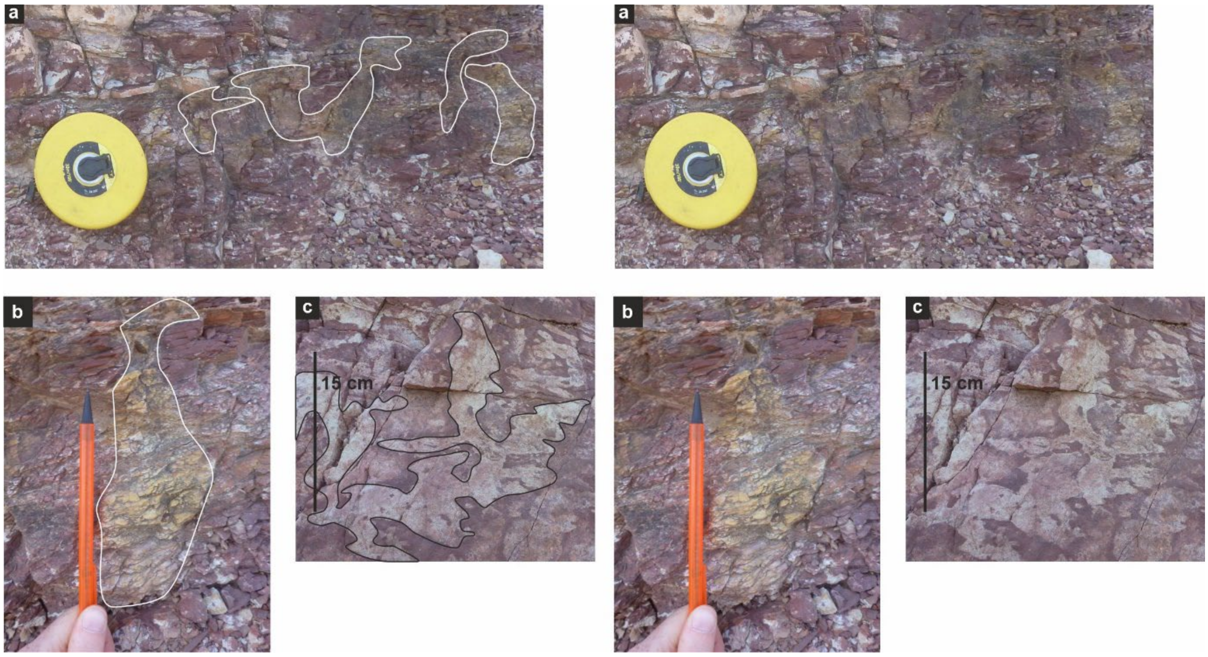

Figure 5: Representative field photographs of colour mottled mudstones and siltstones from the Ghaggar-Hakra Formation (From Beaumont *et al.,*2019), displaying various states of iron oxidation, interpreted as soil horizons with pedogenic products. (A) Typical purple-red mudstones with thin, pale-green siltstone laminae. Small white patches are carbonate nodules, indicating incipient calcrete development. Vertical fabric and associated yellow-brown colour staining result from oxidation of siderite associated with rootlets, originating from beneath the prominent siltstone. The rootlets are sand filled with a carbonised rim preserved. (B) Detail of a vertical branching rootlet and associated iron oxidation, and; (C) irregular branching white reduction zones; on the right-hand side of the figure are un-interpreted versions of each photo.

The outcrops representing the Ghaggar-Hakra Formation are located on the eastern margin of the Barmer Basin and were deposited on a fault-bound relay ramp, oriented northeast-southwest (Bladon *et al.*, 2015). This palaeogeographical context constrains the palaeoflow to the southwest and west (Sisodia & Singh, 2000; Beaumont *et al.,* 2019), and implies a sediment source for this location from the north or northeast. Reported palaeocurrent readings for Lower Cretaceous sandstones throughout the WIRS and LMIB are also to the west and southwest (Table 1), reflecting a regional north-westerly regional palaeo-slope (see also Chaudhuri *et al*., 2018).

Little information is published on the mineralogy and petrography of the Ghaggar-Hakra Formation. Bladon *et al*. (2015b) mention briefly the dominance of sub-rounded monocrystalline and polycrystalline quartz grains and they comment upon a sparse heavy mineral assemblage comprising tourmaline and zircon. The formation is dated to the Albian / Aptian age of the Lower Cretaceous by pollen (c.f. Beaumont *et al*., 2019).

Methodology and sampling

Petrographical samples were collected through each sandstone succession totalling 103 samples through ~200 m of measured and logged succession. A sample was taken each time a change in the grain size occurred vertically through the succession in accordance with the guidelines of Vine & Tourtelot (1970). All samples were thin-sectioned, impregnated with blue-stained epoxy resin to highlight porosity, and examined under a transmitted light petrographical microscope. Of the 103 samples, 50 were chosen for petrographical analysis with 13 samples from the Darjaniyon-ki Dhani Sandstone, 19 from the Sarnoo Sandstone and 18 from the Nosar Sandstone (see supplementary material). Grain size was measured using the Udden-Wentworth grain size classification, across the range from clay to pebble-grade, within the PETROG™ software. 200 grains were point counted using a MicroStepper with PETROG™ using the Gazzi–Dickinson method, and only includes sand-sized grains of 63 microns and above (Dickinson, 1970, 1985; Garzanti, 2019).

Phaneritic and microcrystalline polycrystalline quartz grains are included in the polycrystalline quartz grain category. Quartz or feldspar grains with inclusions of other minerals (including chert) are classified as rock fragments. Igneous rock fragments are classified following Affolter

& Ingersoll (2019) and the metamorphic rock fragments using Garzanti & Vezzoli (2003). Carbonate grains are classified as sedimentary rock fragments. Operator bias was addressed by following the guidelines of Augustsson (2021) and by careful identification of grain types.

The diagenetic history was reconstructed using the burial history of the Ghaggar-Hakra Formation at outcrop, constrained from well data in the Barmer Basin (see Dolson et al., 2015; Naidu et al., 2017) and based on petrographical textural relationships between the diagenetic minerals. From the thin sections, intergranular volume (IGV) was calculated using the methodology from Housenecht (1987) as modified by Ehrenberg (1989). The compactional porosity loss (CoPL) and the total porosity loss due to compaction (XCOM) and original remaining porosity (XPOR) were calculated using the methodology of Ehrenberg (1995) to help further constrain the diagenetic history.

A calculation to reconstruct the original detrital mineralogy was made from the diagenetic sequence as the changes in framework composition and texture that take place during diagenesis can obscure the provenance signal (McBride, 1985; Helmhold, 1985; Harris; 1989 Augustsson, 2021). Feldspar dissolution, during eogenesis or telogenesis, results in the precipitation of feldspar overgrowths, the development of intragranular secondary porosity and precipitation of authigenic kaolinite. For the reconstructions undertaken here, based on our petrographic interpretation of diagenetic processes and following the diagenetic reactions summarised in Worden and Burley (2003) and Augustsson (2021), the original feldspar total is calculated by summation of the totals for feldspar overgrowths, authigenic kaolinite and grain-replacive calcite cement. Aluminium can be mobile during diagenesis (Wilkinson *et al.*, 1996) therefore this reconstruction may underestimate the original detrital feldspar content. Secondary porosity, based on pore shapes and feldspar remnants, is therefore also added to the original feldspar total. Other unstable components, in the case of the Ghaggar-Hakra Formation, finely crystalline lithic fragments with clay alteration that likely were originally mafic minerals, are recalculated by the summation of authigenic chlorite, smectite and indeterminate clay replaced grains to the rock fragment total. Whilst this approach is simple, it does provide an approximation of the original feldspar and mafic rock fragment content of the sandstone at deposition to improve our provenance interpretations.

During mechanical compaction, sedimentary clay clasts, clay-mineral-replaced feldspar and volcanic clasts are ductile and can be compressed to form a pseudo-matrix. This can be mistaken for a detrital matrix and it can cause inappropriate provenance interpretations if not correctly identified. Most of the clays documented here in the Ghaggar-Hakra Formation sandstones are pore-fillings of diagenetic origin.

Of the fifty thin-sectioned samples, 15 were chosen for heavy mineral analysis due to their slightly higher heavy mineral count in thin section. As the sandstones are highly indurated, the samples were initially disaggregated in a coarse mechanical crusher before separation with LST following the procedure detailed by Mange & Maurer (1992). From the 15 samples, seven with the largest heavy mineral fractions were chosen for analysis by Raman Spectroscopy, which usually yields the highest identification precision in heavy mineral analysis (Ando & Garzanti, 2014; Dunkl *et al.,* 2020). The seven samples are from the Darjaniyon-ki Dhani and Nosar sandstones.

Petrography of the Ghaggar-Hakra Formation

Grain size and sorting

Silts and fine sands are well sorted quartzose arenites (Dickinson & Suzeck, 1979; Tucker, 2001). These sediments are typically the cross-bedded and rippled facies of Beaumont *et al*. (2019) and comprise the sandy channel fill sediments. Whereas coarse sands and granules have a poor sorting and are litho-quartzose arenites. These are the bedded and conglomerate facies of Beaumont *et al.* (2019) and comprise the channel lag and basal bedform sediments.

Detrital composition

The detrital composition and texture of the Ghaggar-Hakra sandstones are summarised in Table 2 and plotted on Quartz-Feldspar-Lithic (QFL) diagrams in Figure 6 with representative photomicrographs in Figure 7. Monocrystalline quartz dominates the detrital mode in all sandstones and the modal analysis data indicate that monocrystalline quartz ranges between ~60-80% of all quartz grains (Figure 7a and b). Polycrystalline quartz grains are all coarsely phaneritic, typically well sorted and almost invariably display strained and wavy extinction (Figure 7e). Detrital feldspar is not observed except for in one sample. Although a subordinate component, lithic fragments of igneous, metamorphic and sedimentary origin do occur (Figure 7d and f). Igneous grains are typically dominated by equigranular quartz, with inclusions of other minerals such as muscovite, biotite and monazite, and fall into the vitric or granular categories which correlate to felsic volcanic source rocks (Affolter & Ingersol 2019). Sporadic volcanic grains are present but typically display evidence of partial dissolution and clay replacement that obscure their exact nature. Phenocrysts are rarely observed. Many of these volcanic grains appear to have been microcrystalline or even glassy. Metamorphic grains are mostly schistose and include rigid grains with strong deformation fabrics (Figure 7f). Most are within ranks 1 and 2 of Garzanti & Vezzoli (2003). Sedimentary fragments comprise rigid mudstone clasts (Figure 7c) and, very rarely, dolomitized limestone grains. Sandstone fragments are fine grained and well cemented with authigenic quartz (Figure 7d).

Mineral	Texture and features
Detrital Minerals	
Monocrystalline Quartz	Grain size: from very fine-grained to pebble-grade Shape: sub-rounded to rounded; moderate sphericity Strained: unstrained to slightly strained Contacts: concavo-convex Grain edge corrosion: Locally highly etched by replacive carbonate
Polycrystalline Quartz	Grain size: coarse Shape: sub-rounded, moderately spherical Strained: slightly Contacts: sutured
Sedimentary Rock fragments	Grain size: medium- to very coarse-grained, Shape: sub-rounded Composition: chert Sandstone succession: Darjaniyon-ki Dhani
Igneous Rock fragments	Grain size: coarse-grained Shape: sub-rounded and spherical Composition: quartz with inclusions of muscovite grains Sandstone succession: Nosar
Metamorphic Rock fragments	Grain size: pebble-sized Shape: sub-rounded with a moderate sphericity Composition: sutured, elongated polycrystalline quartz with rough cleavages Sandstone succession: Darjaniyon-ki Dhani
Muscovite mica	Grain size: very fine- to medium-grained Shape: rounded with a very low sphericity; elongated Alteration: expands into the pore spaces and grows dominantly from the rock fragments Birefringence: third order
Pore-filling clays	Grain size: Clay, 50 µm Shape: Sub-angular to sub-rounded and moderately spherical Porosity: detrital pore-filling and grain coating
Authigenic Minerals	

Microcrystalline quartz	Only present in trace amounts
Quartz overgrowths	Features: Small, typically discontinuous, syntaxial. Thickness: up to 2 µm in thickness Single-generation overgrowths
Calcite	Occurrence: fractures in the coarser quartz grains, very occasionally in the pore spaces and as veins cross-cutting other minerals
Dolomite	Occurrence: pores spaces
Kaolinite	Occurrence: Filling intergranular pore spaces and more rarely intergrown with and replacing muscovite mica Shape: Stacked booklets, occasionally vermiform Thickness: 0.5 µm in length
Siderite	Occurrence: filling and choking the pores Shape: fibrous texture Colour: brown
Opaque, iron-rich cements	Occurrence: coats, etches and strains the detrital quartz Features: Circular growths Colour: deep red colour Sandstone succession: Darjaniyon-ki Dhani
Pore types	
Primary porosity	Grain size: Fine-grained Shape: moderately spherical % of pore space counted during point counting: Darjaniyon-ki Dhani: 3.25% Sarnoo: 3.38% Nosar: 3.68%
Secondary porosity	Grain size: Coarse-grained Shape: moderately spherical % of pore space counted during point counting: Darjaniyon-ki Dhani: 2.61% Sarnoo: 3.05% Nosar: 4.75%

Table 2: Summary of detrital and authigenic textures and mineral composition of the Ghaggar-Hakra sandstones studied in thin section (Figure 7).

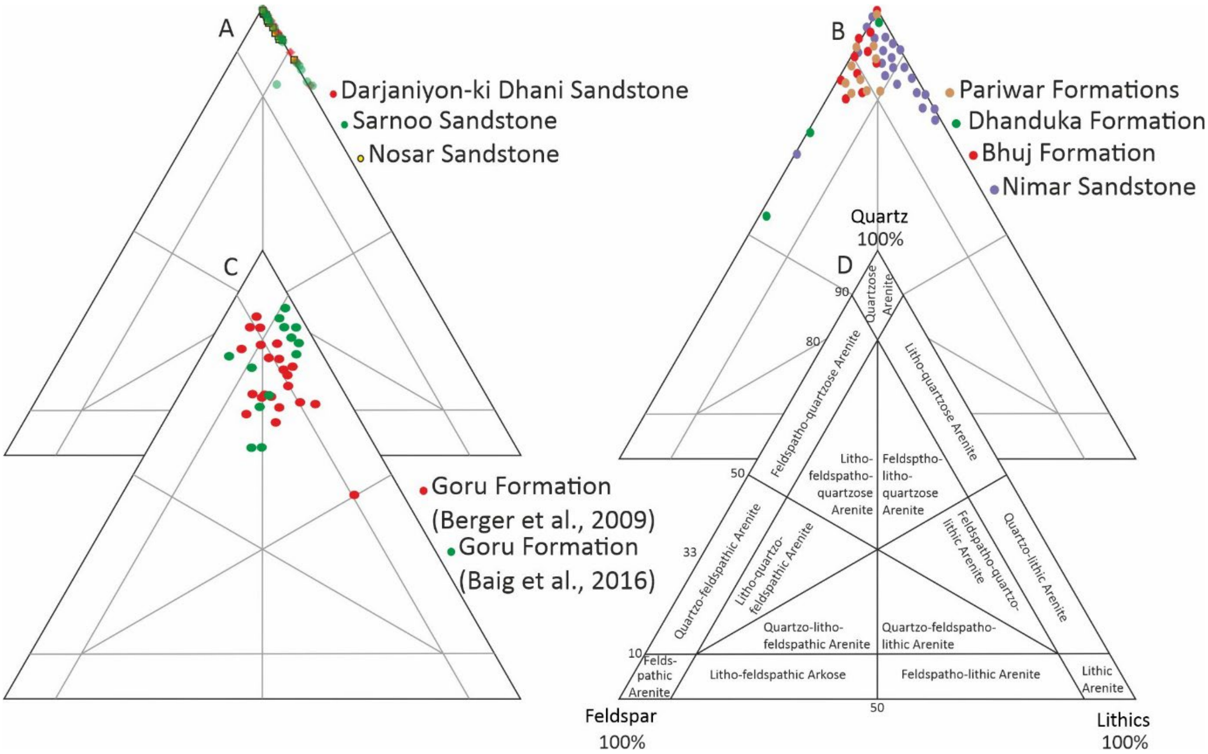

Figure 6: QFL detrital composition plots of the current detrital mineralogy of the (A) Ghaggar-Hakra Formation sandstones compared with QFL plots from elsewhere: (B) WIRS (Cambay Basin: Aquil, 1982; other basins: Racey *et al.,* 2016) and the (C) LMIB sandstones from the literature (Berger *et al.,* 2009; Baig *et al.,* 2016). D displays the classification scheme from the Gazzi-Dickinson method, further developed by Garzanti (2019).

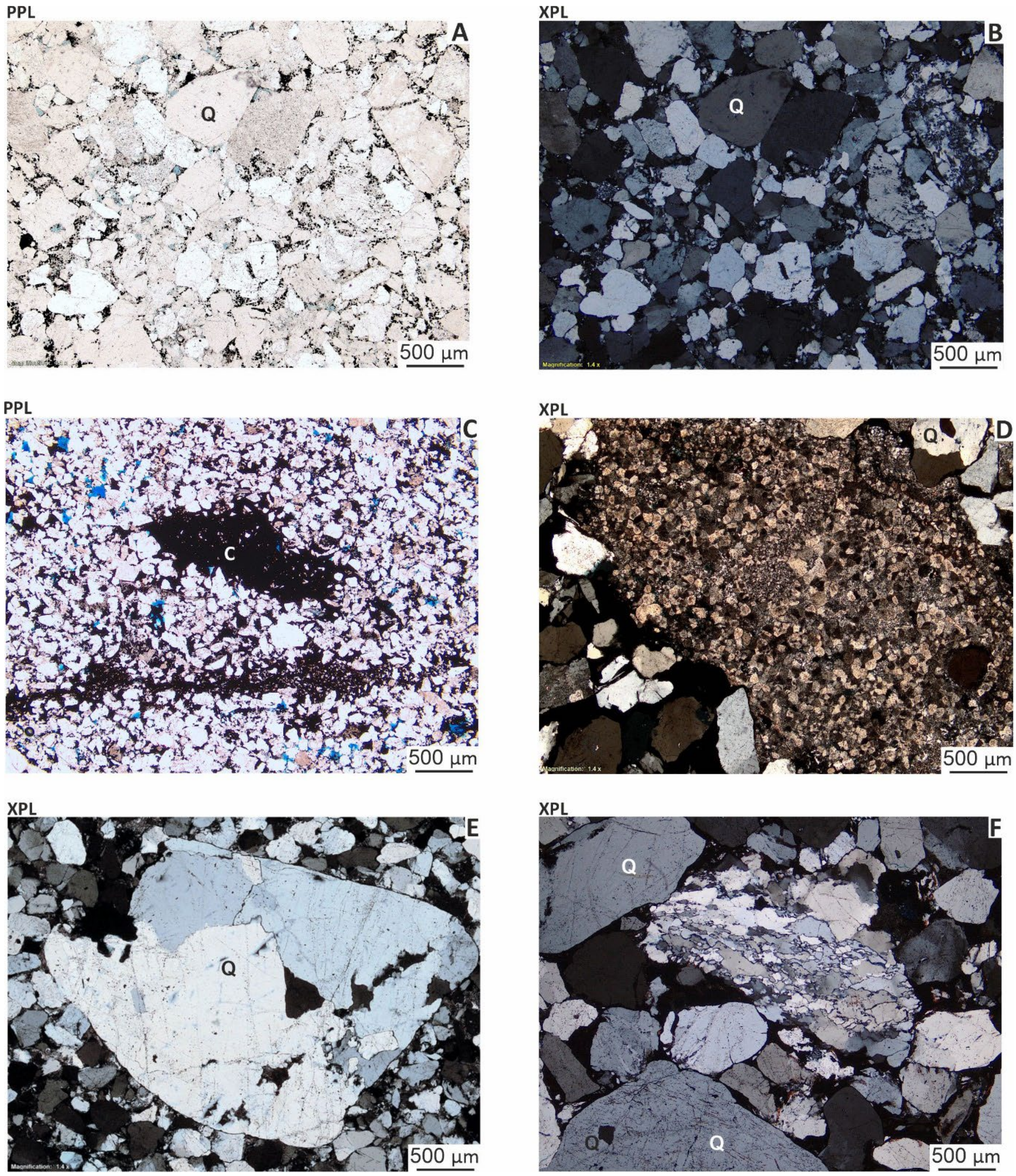

Figure 7: Representative photomicrographs of the Ghaggar-Hakra Formation at outcrop; scales on micrographs. (A & B) Plane-polarised and cross-polarised pair showing the typical texture and mineralogy of coarse-grained sandstones. Note the poor sorting, well rounded grains dominated by monocrystalline quartz, with only subordinate polycrystalline quartz; (C) Example of a sedimentary mudstone rock fragment, probably an intraclast; (D) Unusual sandstone rock fragment cemented with quartz overgrowths; (E) Typical polycrystalline quartz grain (Q), and; (F) Typical schistose quartz grain of probable metamorphic origin. Blue colour in PPL micrographs is the epoxy used to impregnate the

sandstones for thin section preparation and displays porosity; where Q = Quartz, C = Mudstone intraclast.

The heavy mineral assemblage comprises tourmaline, zircon, rutile, staurolite, baryte and a suite of indeterminate, generally poorly reflective, opaque minerals (Table 3 and Figures 8 & 9). Authigenic TiO_2 polymorphs anatase and brookite occur frequently and anatase represents the most abundant translucent heavy mineral. Opaque grains dominate the total heavy mineral assemblage, and whilst a few retain strongly reflective cores, suggestive of ilmenite or magnetite, most are highly oxidised and their red-coloured reflectivity, semi-transparent nature indicates that they are now finely crystalline haematite. Rutile and tourmaline dominate the translucent non-diagenetic heavy mineral assemblage in most of the samples, whilst staurolite is a significant component in one sample from the Nosar Sandstone. Due to the high number of authigenic anatase and the abundance of opaque minerals, the count numbers for non-diagenetic heavy minerals are below the 200-300 counts for statistical determination (Mange & Maurer, 1992; Garzanti *et al.,* 2014). The Darjanyon-ki Dhani Sandstone is dominated by rutile and baryte, while the younger Nosar Sandstone yields tourmaline, baryte, staurolite, rutile and zircon. . Most samples have also several carbonate minerals in their heavy mineral assemblage.

Mineral	**Transmitted light colour**	**Grain size**	**Shape**	**Other**
Tourmaline	Blue, pink, brown	Fine to medium-grained	Subhedral, blocky in appearance, up to, sub-angular to sub-rounded with a high sphericity	Pleochroic, high-order birefringence colours
Zircons	Transparent	Fine-grained	Rounded with a high sphericity	Third-order birefringence colours
Rutile	Brown	Fine to medium-grained	Rounded, with a low sphericity, thin and elongated	Third-order birefringence colours
Baryte	Pale yellow	Coarse-grained	Angular to sub-angular with a medium sphericity	Low, first order greys to second-order yellow, turbid appearance
Staurolite	Yellow	Fine- to medium-grained	Sub-rounded with a high sphericity	Pleochroic, platy grains, inclusions
Opaques	Opaque	Ranges from fine-	In general: sub-rounded with a low sphericity	N.A.

		to coarse grained		

Table 3: Summary of optical characteristics of heavy mineral grains.

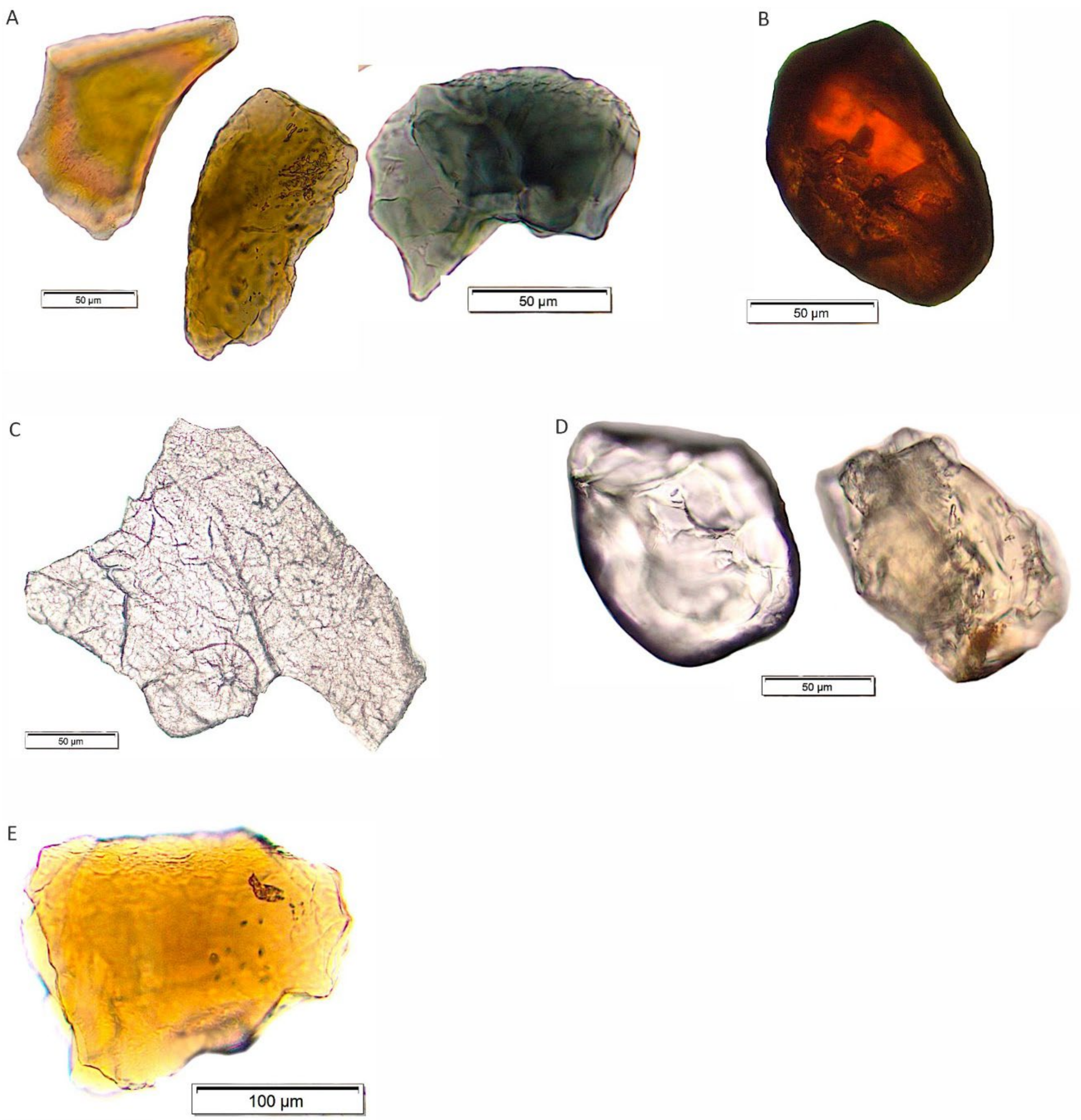

Figure 8: Optical light photomicrographs of representative non-embedded, unmounted, viewed in air heavy mineral grains from the Ghaggar-Hakra Formation showing their typical appearance. All micrographs in transmitted PPL; scales shown on photographs. (A) Tourmaline and its 3 distinct colours, from left to right: pink, brown and blue; (B) Rutile; (C) Baryte; (D) Zircon, and (E) Staurolite.

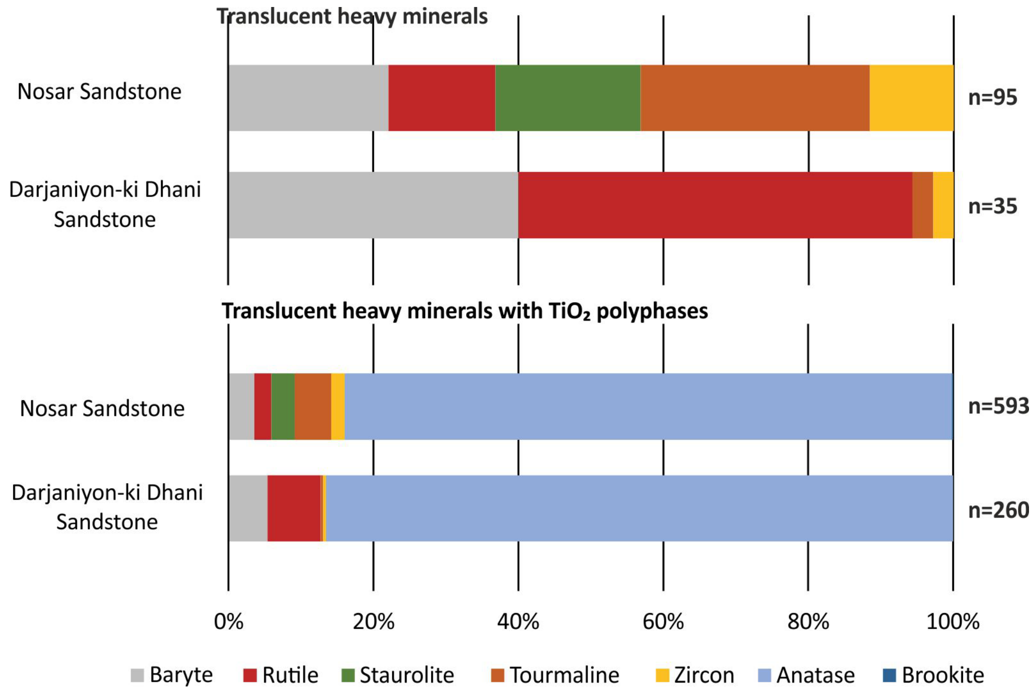

Figure 9: Summary of the proportion of mineral species in seven samples determined by Raman Spectroscopy on heavy mineral concentrates. The dominance of tourmaline and rutile, but staurolite, suggest a metapelite provenance. Baryte in samples 73 and 94 is present as a pore-filling cement, which may have formed during early diagenesis. (A) Translucent heavy minerals counts, and; (B) Translucent heavy mineral counts with TiO_2 polyphases.

Diagenetic textures and mineralogy

The Ghaggar-Hakra Formation has undergone a complex diagenetic history which is difficult to unravel from textural relationships alone. Constructing a burial history (Figure 10) places some constraints on the timing of diagenetic events which helps qualitatively resolve the diagenetic sequence. The most striking petrographical characteristic is the extreme mechanical compaction fabric (Figure 11a) which affects most samples. Grain re-orientation and brittle fracturing of individual detrital grains across fulcrum points are very pronounced and long or indented grain contacts are typical. Sutured quartz grain contacts are rare, indicating pressure dissolution has not been important. Calculations of intergranular volumes (IGV) for matrix-free sandstones averages at 18% supporting observations that mechanical compaction has had the largest effect on porosity loss (Figure 12a). Lowest values of IGV are associated with highly compacted, poorly sorted sandstones. The average intergranular volumes within the sandstones are 27% for the Darjaniyon-ki Dhani, 18% for the Sarnoo, and 12% for the Nosar.

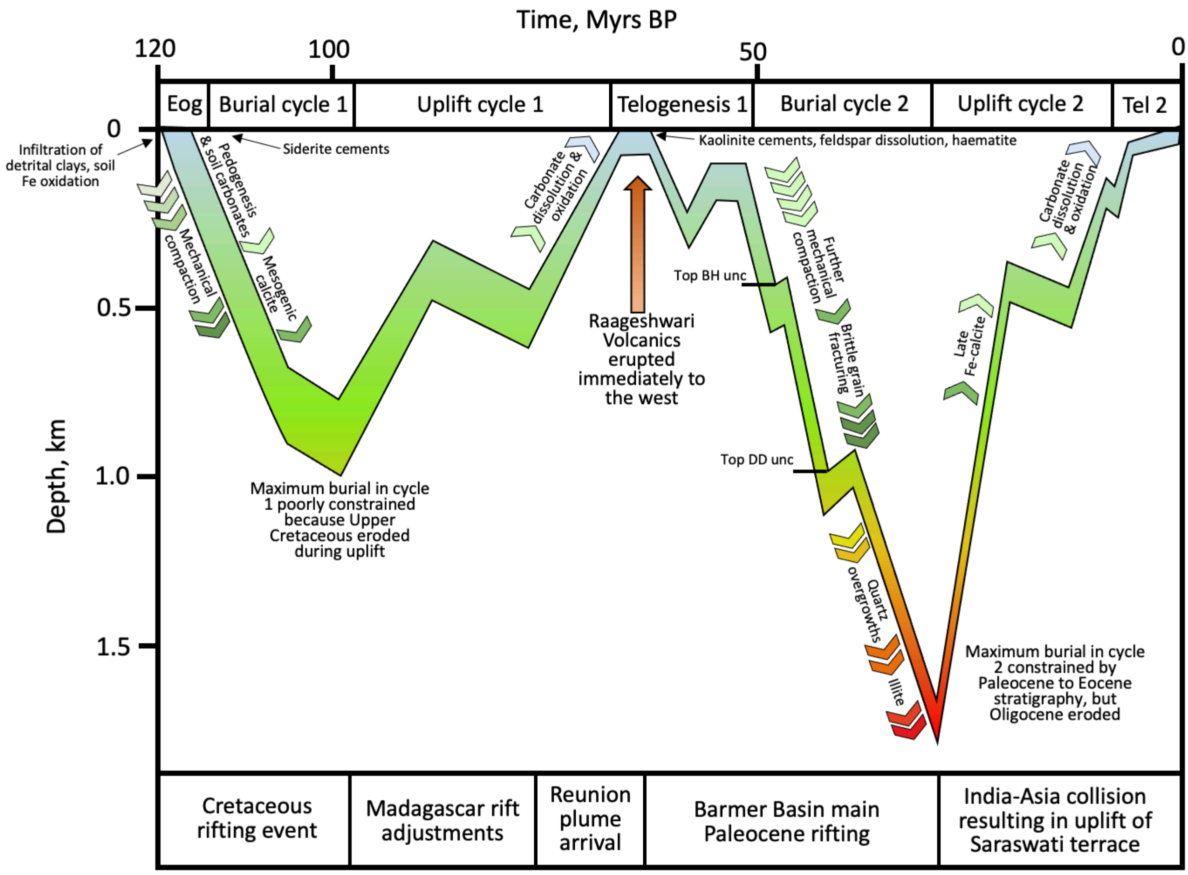

Figure 10: Paragenetic sequence of diagenetic events in the Ghaggar-Hakra Formation based on thin section petrography for quartz-rich sandstones and soil profiles in the context of the burial history curve for the outcrop sequences. Maximum burial in the Cretaceous Period is poorly constrained because the Upper Cretaceous sequence is widely eroded across the WIRS, but consideration of stratigraphic sequences indicates that the Cretaceous strata is unlikely to have exceeded 1 km of total thickness. Deepest burial took place in the Palaeocene-Eocene in the Barmer Basin (Dolson *et al.,* 2015; Naidu *et al.,* 2017) prior to regional uplift due second stage Himalayan formation (Najman, *et al.,* 2018; Powell & Conaghan, 1973). Eog = eogenetic, Tel = teleogenesis.

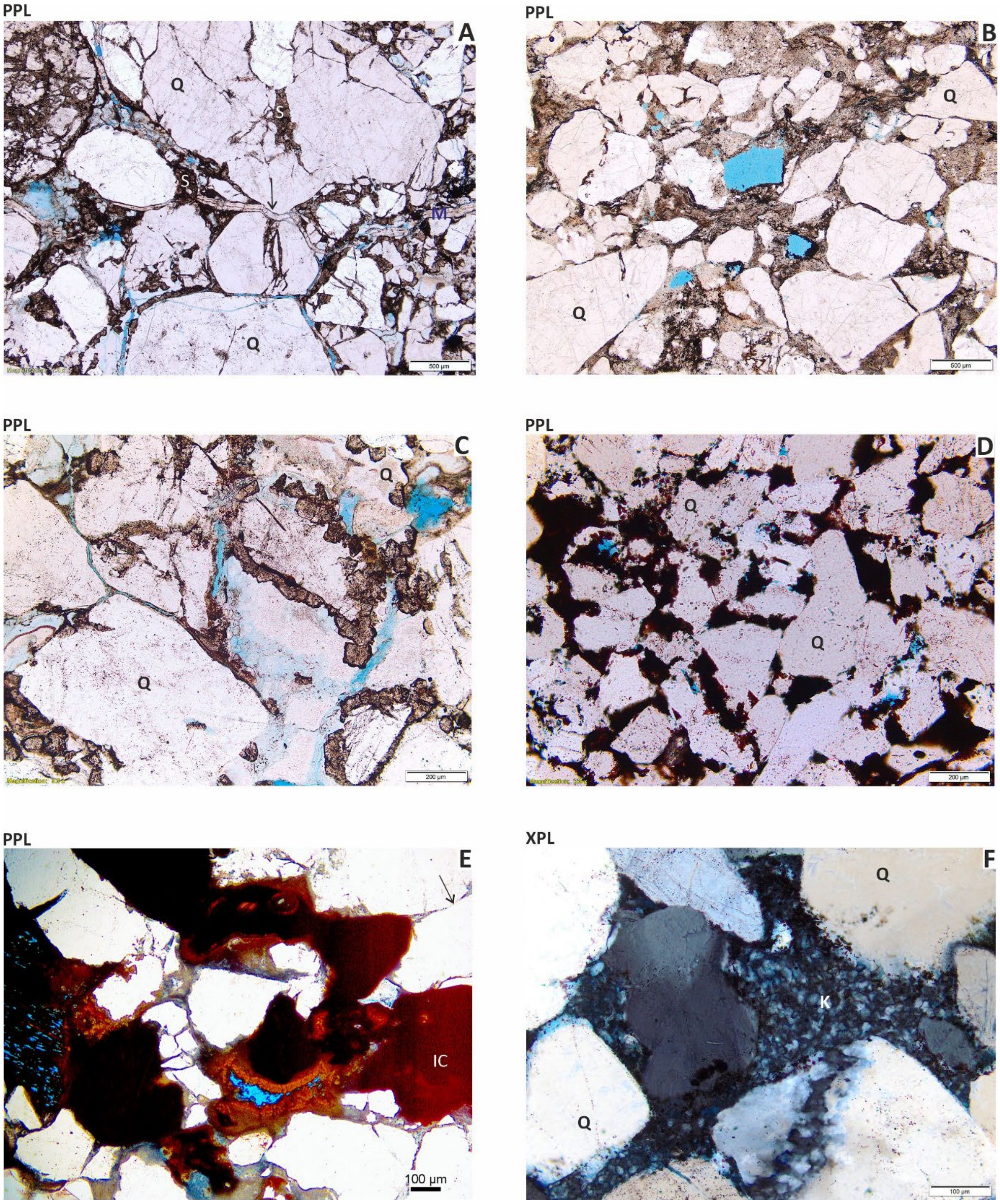

Figure 11: Representative photomicrographs of the Ghaggar-Hakra Formation showing diagenetic features; scales on micrographs. (A) Detail of the mechanical compaction fabric with crushed and splintered grains, indicated by arrow; (B) Oversized, secondary grain dissolution pores in a coarsely crystalline calcite cemented sandstone. Note the compaction fabric despite the carbonate cement; (C) Grain-rimming early siderite cement with an outer oxidation rim; (D) Pervasive oxidation of pore filling and grain replacive siderite cement; (E) Detail of oxidized siderite, and; (F) Pore-filling authigenic

kaolinite cement. Blue colour in PPL micrographs is the epoxy used to impregnate the sandstones for thin section preparation. Where: Q – Quartz; S – Siderite; IC – Iron cements, and K – Kaolinite.

Sandstones associated with soil horizons contain grain rimming siderite and sparry calcite cement enclosing the siderite, which both preserve IGV (Figures 11b, 11c & 11e). This siderite and enclosing calcite must therefore have precipitated prior to mechanical compaction. Although now optically haematite, many of these textures are reminiscent of the early siderite cements and are interpreted in the modal analysis as oxidised siderite cement. The contrast between sandstones with early carbonate cements and those without is clearly shown Figure 12b. The early carbonate cement has stopped extreme mechanical compaction due to rigidity provided by carbonate cements. The plot of XPOR vs XCOM (Figure 12c) indicates that the Ghaggar-Hakra Formation records the end-product of extensive mechanical compaction, most probably the result of rapid burial in the Palaeocene Epoch. Except for sandstones with early carbonate cements, most of the porosity loss resulted from mechanical compaction.

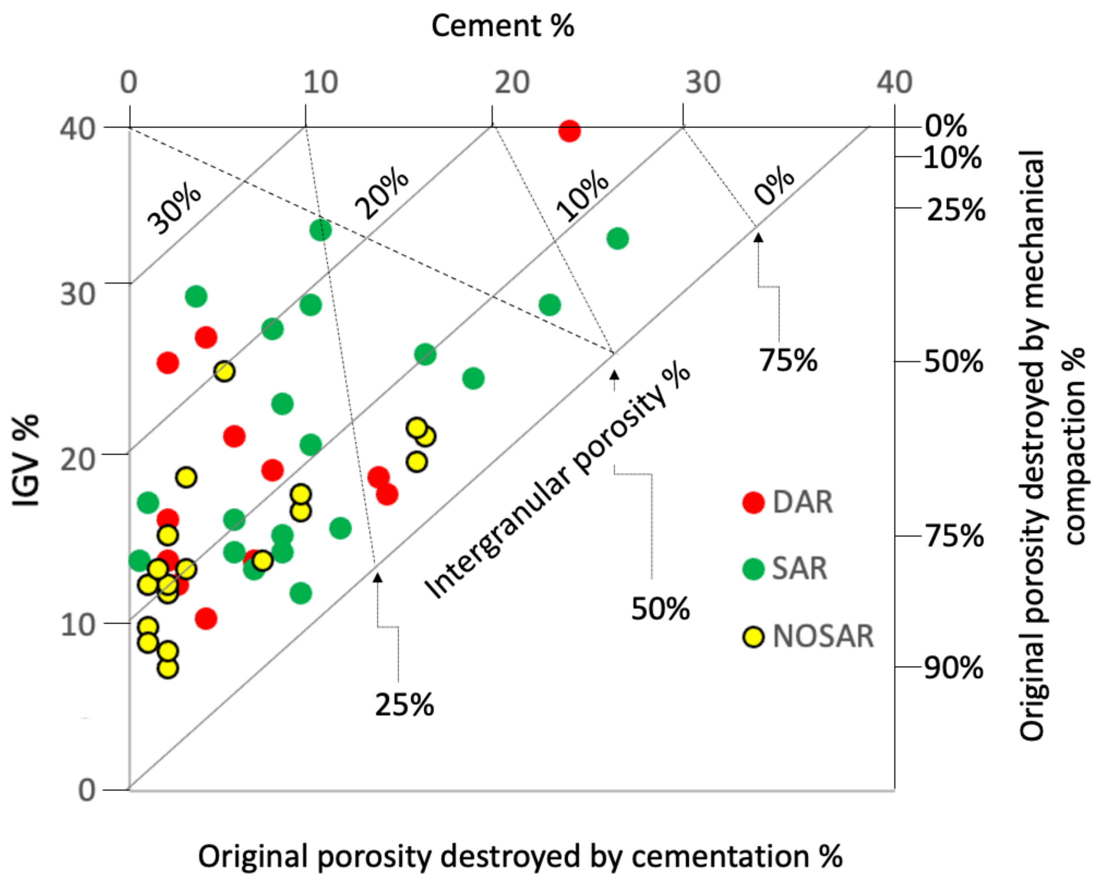

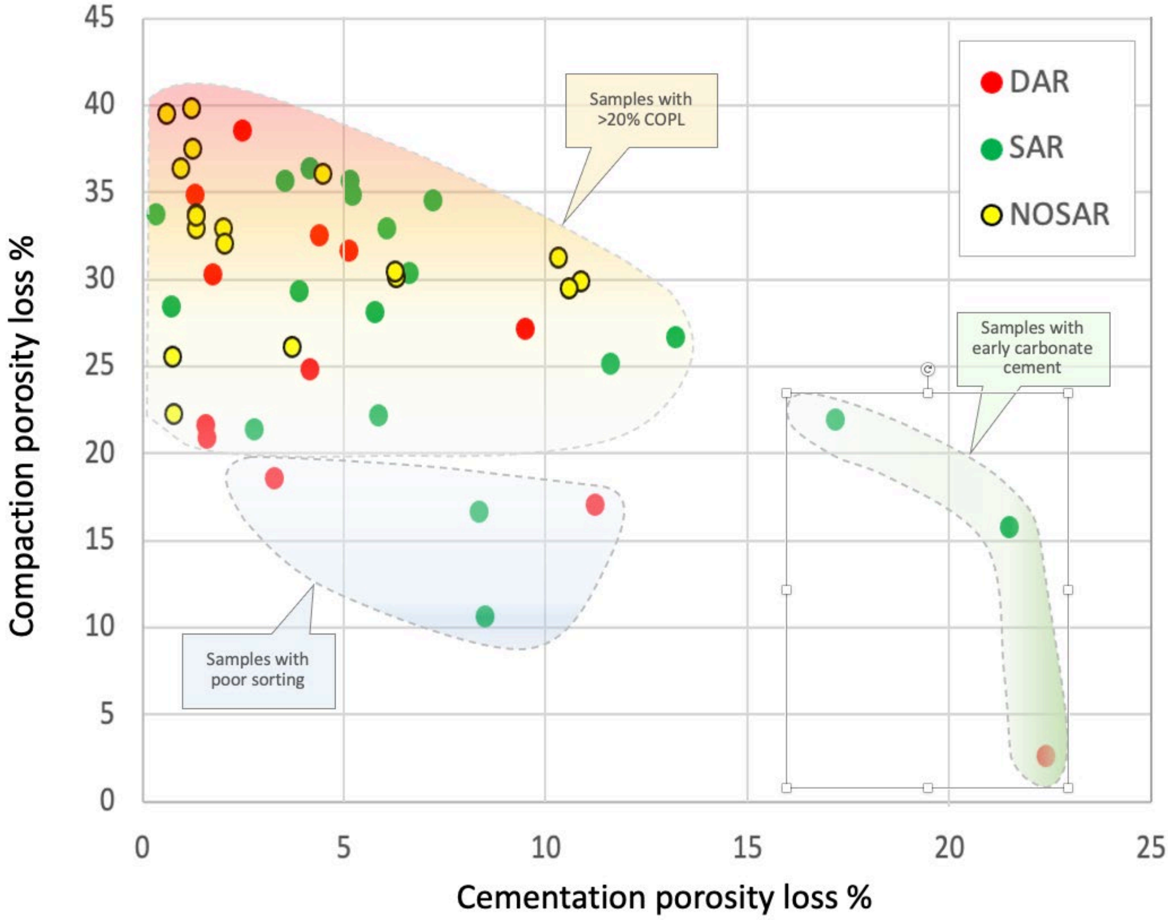

45
40
35
30
25
20
15
10
5
0
Compaction porosity loss %
0
5
10
15
20
25
Cementation porosity loss %
DAR
SAR
NOSAR
Samples with >20% COPL
Samples with early carbonate cement
Samples with poor sorting

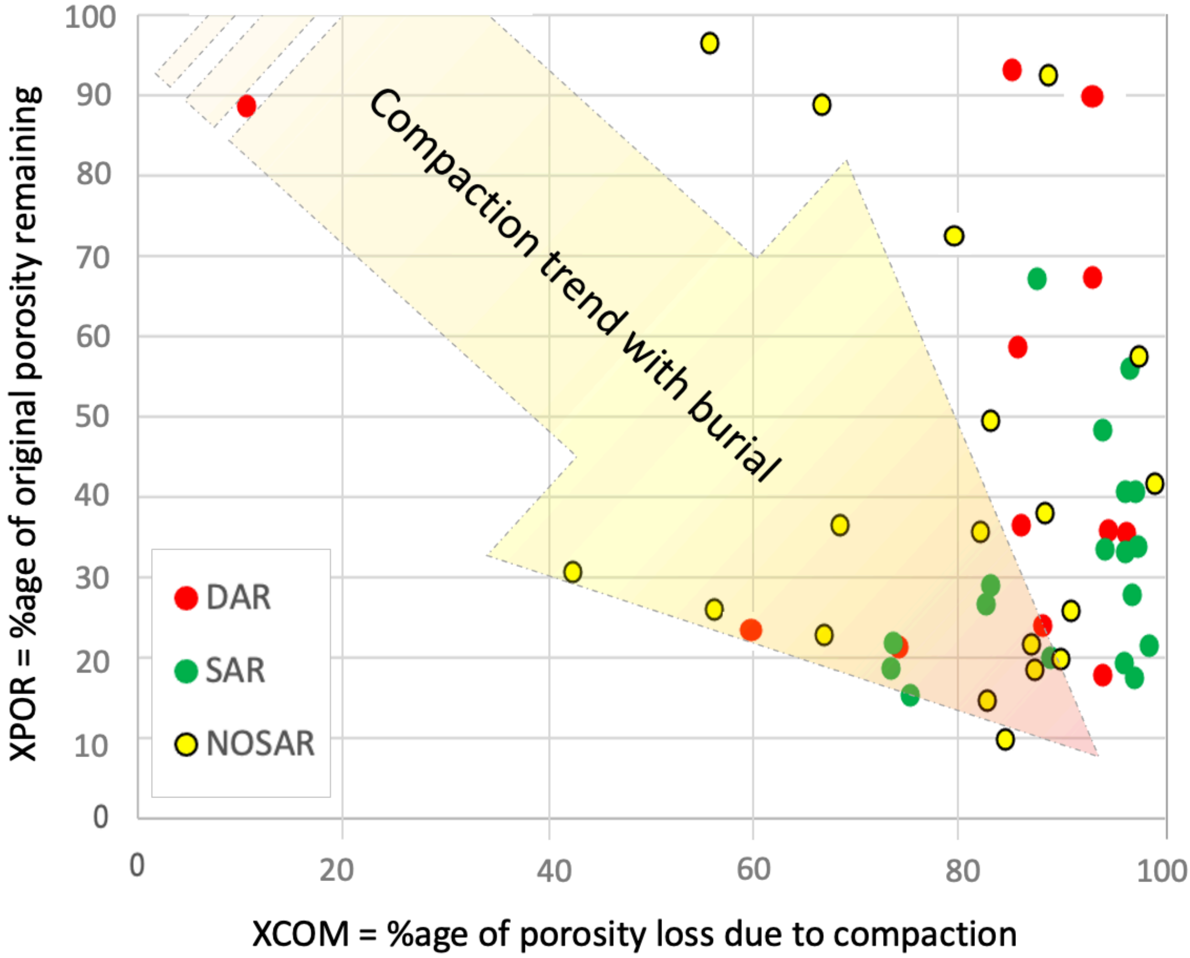

Figure 12A: Percentage IGV plotted against intergranular cement determined from thin section modal analysis using the Ehrenberg (1989) modification of the Housenecht (1987) calculations. Most samples have low IGV with most original porosity being destroyed by mechanical compaction. Three samples with >30% IGV contain early carbonate cements. **(B)** Graph of percentage compactional porosity loss (COPL) and porosity loss by cementation (CEPL) in the Ghaggar-Hakra Formation sandstones highlighting the main groupings. Except for sandstones with early carbonate cements, most porosity loss is from mechanical compaction. COPL and CEPL calculations from Ehrenberg (1995). **(C)** Graph of percentage of porosity loss due to compaction (XCOM) against the percentage of original porosity remaining (XPOR). The data indicates that the Ghaggar-Hakra sandstones record the end product of extensive mechanical compaction, consistent with the COPL vs CEPL plot, most likely the result of rapid burial in the Paleocene. Sandstones retaining a high percentage of original porosity contain early carbonate cements. Calculations of XCOM and XPOR from Ehrenberg (1995). Legend on all graphs: DAR – Darjaniyon-ki Dhani Sandstone; SAR – Sarnoo Sandstone and NOSAR – Nosar Sandstone.

Well-sorted sandstones typically display the presence of oversized pores, many of which contain authigenic kaolinite (Figure 11f) and in places may be cemented with later carbonate

(Figure 11b). For this reason, it is likely that intense feldspar grain dissolution took place at the end of the Cretaceous Period when the Ghaggar-Hakra Formation was subaerially exposed, prior to Palaeocene burial. Maximum burial took place in the Late Eocene or Early Oligocene epochs and reached almost 2 km depth (Figure 10) before uplift related to the second stage of the Himalayan formation (Najman *et al.*, 2018; Powell & Conaghan, 1973) causing minor basin inversion.

<u>Original detrital mineralogy</u>

An attempt to remove the diagenetic effects on the modal detrital composition has been undertaken by restoring diagenetic products to the detrital mineralogy. Grain replacive calcite cement, authigenic kaolinite and oversized pores are added together with the feldspar content to calculate the potential original feldspar. Summation of authigenic chlorite, smectite and indeterminate clay-rich grains plus the observed lithics provides an approximation of the original lithics total.

The recalculated (see supplementary material) detrital composition indicates that the Ghaggar-Hakra Formation compositionally remains dominantly quartzose arenites (Figure 13) with relatively low feldspar-contents. The same calculation has also been completed on data for the WIRS and the LMIB for comparisons (Figure 13) and overall provenance estimations.

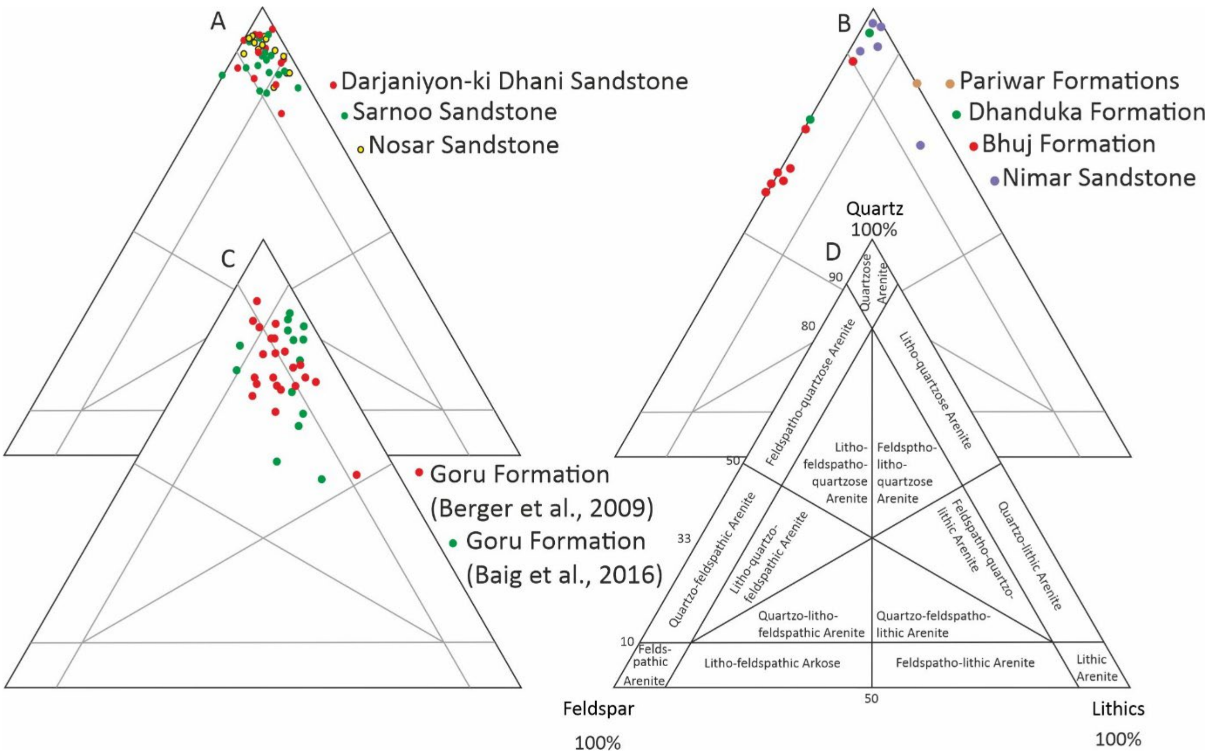

Figure 13: QFL diagrams for the reconstructed detrital mineralogies including feldspar as explained in the text; A) The Ghaggar-Hakra Formation; B) Other basins in the WIRS from Aquil (1982) and Racey *et al.,* (2016); C) The LMIB from Berger *et al.,* (2009) and Baig *et al.,* (2016). Comparison of these data with the original QFL data from Figure 6 (A) the Ghaggar-Hakra Formation clearly indicates a significant increase in feldspar, particularly within the Nosar Sandstone; (B) the WIRS largely appears the same apart from the Bhuj Formation of the Kachchh Basin which shows a reduction in lithic fragments; (C) The Goru Sandstone of the LMIBs show an increase in lithic fragments overall, D on both figures displays the classification scheme from the Gazzi-Dickinson method, further developed by Garzanti (2019).

Interpretation

<u>Effects of diagenesis on the Ghaggar-Hakra detrital minerals</u>

The specific timing of diagenetic events is difficult to constrain, which has a bearing on the relative importance of weathering or diagenesis on the detrital mineralogy. The earliest diagenetic processes preserved at outcrop are related to soil formation and infiltration of clay (Diko, 2013) which must be of Early Cretaceous age. Optical petrography indicates that the earliest carbonate cements were siderites, which display extensive oxidation to haematite. This oxidation could be related to the Lower Cretaceous soil formation (Driese *et al*., 1995; Salama & Anand, 2017) or subsequent uplift at the end Cretaceous Period, or present-day climatic conditions. Given that both siderite and calcite remain preserved at outcrop, our preferred interpretation is that the siderite oxidation is related to Lower Cretaceous soil development.

During the initial burial cycle (Figure 10) calcite cements enclose the soil carbonates and were precipitated as mechanical compaction progressed. The end of this first burial cycle is poorly constrained, but it is likely to have occurred at around 1 km depth based on known thicknesses of Lower Cretaceous sediments in WIRS (~700 m in Ramgarh-1 in the Jaisalmer Basin, NDR database, 2021; maximum 1800 m of Cretaceous recorded in the Jaisalmer Basin, Zadan & Arbab, 2015; <200 m on the Saraswati Terrace, Barmer Basin, Dolson *et al*., 2015). Strata were then subaerially exposed at the end Cretaceous Period when the main Palaeocene rifting in the Barmer Basin took place (Dolson *et al*., 2015; Vijayan *et al*., 2016; Naidu *et al*., 2017; Millett *et al*., 2021; Sharma *et al*., 2021). Although it is not possible to be definitive regarding the extent of diagenesis at this unconformity surface, the uplift was of long duration and resulted in the removal of all Upper Cretaceous sediments (Sheth, 2007). Consequently, it is probable that dissolution of carbonate, unstable volcanic lithic fragments and feldspars (forming oversized pores), and precipitation of authigenic kaolinite, took place during this exposure.

Petrographical observations indicate that the second burial cycle principally comprised further mechanical compaction followed by quartz cementation, with little evidence of grain removal. Rapid Palaeocene burial suggests that this is when most of the brittle grain fracturing and mechanical compaction took place. Compacted oversized pores suggest most grain dissolution had taken place prior to burial. Precipitation of microcrystalline quartz and quartz overgrowths into both the primary and secondary pore spaces indicate precipitation of these cements occurred after the dissolution of unstable grains. Illite replacement of kaolinite takes place at temperatures of >120°C (Bjorkum & Gjelsvik, 1988) suggesting that the second burial cycle attained depths approaching 2 km.

Uplift that produced the present-day outcrop occurred rapidly, due to the Indian-Asian collision (Naidu, *et al.,* 2017). Calcite dissolution and oxidation are interpreted to be associated with aforementioned uplift , but in a grain framework which was already altered by earlier diagenetic processes. The QFL diagrams for the reconstructed detrital mineralogies (Figure 13) indicate that allowing for all the observed diagenetic processes the composition of the Ghaggar-Hakra Formation remains largely quartzose arenite, even though there is a small increase in detrital feldspar content. The regional view of the WIRS shows a distinct increase in feldspar content, particularly in the sediments of the Bhuj Formation of the Kachchh Basin which also display an increase in abundance of lithic fragments. The Lower Goru Sandstones of the LMIBs show an overall increase in lithic fragments and feldspar (Figure 13).

Heavy mineral analysis of the Ghaggar-Hakra Formation documents that the Darjaniyon-ki Dhani and Nosar sandstones are dominated by stable rutile and tourmaline which are resistant to weathering. Rutile dominates in the Darjaniyon-ki Dhani Sandstone, while tourmaline becomes more abundant in the Nosar Sandstone, where staurolite also occurs.

An assemblage consisting of predominantly rutile, tourmaline and staurolite with zircon being less abundant, is typical of a metapelite protolith (Henry & Guidotti, 1985; Moton & Chenery, 2009; Kotowski *et al*., 2020). The zircons are dated to 750-880 Ma within the Kachchh Basin therefore are likely to be from the Malani Igneous Suite (c.f. Chaudhuri *et al*., 2020b). The age and the observed well-rounding of the heavy minerals suggest they were likely recycled multiple times whereas the sand grains of the Ghaggar-Hakra Formation were sourced by recycling of older sedimentary successions. The baryte probably represents cement formed during soil formation and may be related to feldspar dissolution in the Darjaniyon-ki Dhani and Sarnoo floodplains (Jennings *et al*., 2015). Minerals that are susceptible to acid dissolution, such as garnet and apatite, are completely absent from the sandstones, probably due to diagenesis or to prolonged subaerial exposure in a fluvial environment (Morton, 1986; Morton & Hurst, 1995). Similarly, the other metamorphic index heavy minerals andalusite, kyanite and sillimanite, which are unstable during deep burial (Morton, 1985), are also missing from the assemblage. The abundant authigenic anatase, which forms overgrowths on detrital grains, is probably associated with the second deeper burial phase. The available count numbers are unfortunately not enough to distinguish confidently between the different sandstones of the Ghaggar-Hakra Formation but the occurrence of staurolite in the Nosar Sandstone and the high abundance of rutile in the Darjaniyon-ki Dhani Sandstone could suggest slightly different sources. More research on heavy minerals is needed.

Ghaggar-Hakra Formation provenance: provenance composition or climate?

The sandstones are dominated by quartzose arenites containing little feldspar or lithics, even when the effects of diagenetic modification for the depositional location are considered. Undoubtedly, diagenetic processes have modified the original detrital composition, but there is insufficient evidence to reconstruct the granitic and lithic compositions expected from the potential provenance domains. This leaves either extreme weathering in the provenance area, or the Ghaggar-Hakra sandstones are at least second-cycle sediments (Blatt, 1982; Dickinson, 1985; Akhtar & Ahmad, 1991). The occurrence of heavy minerals (zircon, tourmaline and rutile: ZTR) is also consistent with either of these processes (Blatt, 1982; Moral Cardona *et al*., 1997). The dominance of ZTR is typical for multi-recycled sedimentary sources (Hubert, 1962). It is difficult to justify breakdown of other less-stable heavy minerals by weathering at the original source or by very strong diagenetic processes (acidic leaching and deep burial-related dissolution). The burial and uplift history of the Ghaggar-Hakra Formation (Figure 10) provides some constrains on the maximum depth of burial or duration of subaerial exposure. Given the sparsity of quartz overgrowth cements and pressure dissolution, burial to temperatures much greater than 80°C is unlikely, and not supported by stratigraphical considerations.

Palaeogeographical reconstructions indicate that the depositional location of northwest India in the Lower Cretaceous Epoch was approximately 40° south of the equator where modelling indicates it would have been a subtropical to temperate seasonal climate with mean annual temperatures around 17°C (Scotese *et al*., 2007; Goswami, 2011; Scotese, 2011) and with relatively low precipitation rates (1.5 – 12 cm/month; Hallam, 1985; Chatterjee *et al*., 2013; Ali & Aitchison, 2014; Chopparapu & Rajanikanth, 2018). The depositional climate was thus dry and temperate. This palaeo-climate is inconsistent with deep weathering capable of producing a residual quartz mineralogy in the provenance areas (c.f. Bata *et al*., 2016; Rahman *et al.,* 2021) and there are no records of Early Cretaceous lateritic deposits in northwest India, unlike in the Late Cretaceous and Palaeocene periods when widespread laterites and duricrusts developed (Widdowson, 1997). Suttner *et al*. (1981) argues that under these conditions intense chemical weathering to produce first-cycle quartz arenites is highly unlikely. In addition, the composition of the Ghaggar-Hakra Formation falls in the interior cratons / recycled quartzose areas of the Dickinson *et al.* (1983) provenance plot (Figure 13A).

An alternative to extreme chemical weathering is that these sandstones are multi-cycle derived at least in part from pre-existing sandstones. The main candidate is the Marwar Supergroup deposited in large intracratonic basins (McKenzie *et al*., 2011). The Marwar Supergroup contains the Jodhpur Group which is a succession that is >1 km thick and consists of fine- to coarse-grained quartz arenites with very small amounts of quartz overgrowth cement (Kumar *et al*., 2011), deposited within mostly fluvial settings (George & Ray, 2017). This group unconformably overlies and covers much of the Malani Igneous Suite providing a potential explanation as to why there are very few volcanic lithoclasts in the Ghaggar-Hakra Formation: the Malani Igneous Suite was simply covered by the Jodhpur Group in the Lower Cretaceous Epoch. Given that the sandstones of Jodhpur Group are quartzose arenites they are consistent with being a contributory source for the Ghaggar-Hakra Formation.

Furthermore, quartz arenites of the Jurassic Lathi Formation also blanketed large areas of the northern Barmer Basin and flanking basement rocks into the Cretaceous (Ahmad *et al*., 2000) which are also polycyclic quartz arenites (Alam *et al.,* 2000).

Comparison with other sandstones of the WIRS & LMIB

The detrital mineralogy of all Lower Cretaceous sediments indicates a general increase in feldspar and a decrease in quartz from east to west (Figure 13) across the northern Indian Plate. Sediments of the Cambay Basin were derived from an interior craton, sediments from the Jaisalmer Basin were derived from a recycled orogeny, whilst those from the Narmada Basin were derived from both an interior basement craton / recycled sediment (Figure 13B). By contrast, the sandstones of the Bhuj Formation of Kachchh Basin were derived from a recycled orogen and a transitional continental basement, mostly probably the Saurasthra High or Pachham High (c.f. Beaumont *et al.,* 2019). Sediments in the Lower Indus Basin were locally derived from the flanking highs whilst those of the Middle/Upper Indus Basin are derived from dissected arcs and recycled orogens (Figure 14; Beaumont *et al.,* 2019). The findings indicate Lower Cretaceous fluvial systems supplying the Narmada, Cambay, Barmer, Jaisalmer and Upper/Middle Indus basins ultimately derived detrital materials from within the Aravalli Range and have transport paths which flow across extensive exposures of the Jodhpur Group and probably Lathi Formation (Figure 14).

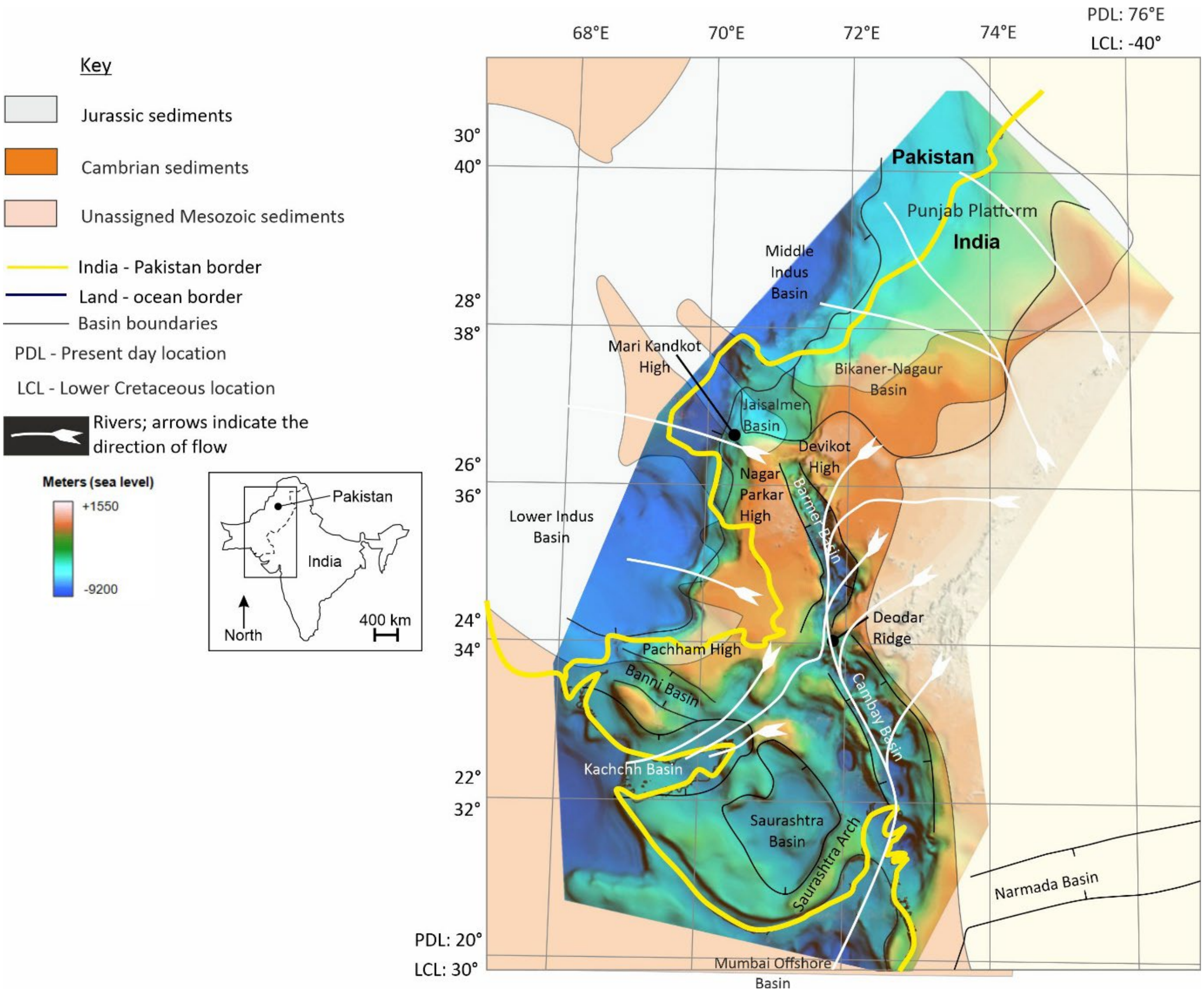

Figure 14: Palaeogeographical reconstruction showing the provenance terrains exposed across the northern Indian Plate in the Lower Cretaceous Epoch able to provide detritus to the Cretaceous depositional systems. The underlying data has a depth to top basement map which is calibrated with gravity and magnetic data which has been linked with seismic and well data for the Barmer Basin (Kothari *et al.,* 2015; Dolson *et al.,* 2015).

Distinguishing between first- and multi-cycle quartzose arenites is difficult as sediment derived from one provenance terrain is remobilized and mixed with sediment from other sources, resulting in the diagnostic characteristics of their provenance being obscured (von Eynatten & Dunkl, 2012). Typically, multi-cycle arenites include recycled quartz overgrowths (Basu *et al*., 2013) and potentially transported fluid inclusions (Haile *et al*., 2021) but there is no evidence of these in the Ghaggar-Hakra Formation. This is not surprising, as the proposed earlier provenance reservoirs (Jodhpur Group and Lathi Formation) contain few quartz overgrowths. However, Chaudhuri *et al.* (2018; 2020b) document the presence of transported quartz overgrowths in Cretaceous sandstones from Kachchh supporting the polycyclic nature of these sediments from a pre-Jurassic basin. The limited petrographic data from the Sonia Sandstones of the Jodhpur supergroup are reported to contain only small quartz overgrowths (Kumar et al., 2011) which may not have survived transport whilst the Lathi Formation is devoid of quartz overgrowths (Alam et al., 2000). Further to this we observe a highly rounded nature to the heavy minerals as does Chaudhuri *et al.,* (2018) in the Kachchh Basin, where the zircons are likely to have been recycled, potentially multiple times by being reworked in the Cambrian and then again in the Cretaceous based on their age (George & Roy, 2017). The Palaeoproterozoic and Archean zircons surely would come originally from the Aravalli or Singhbhum cratons. The zircons have been recycled many times into sedimentary strata that has been eroded and deposited in the Kachchh (Chaudhuri *et al.* 2018; 2020b). First-cycle quartz-arenites typically develop there is intense chemical weathering or they generally contain higher counts of lithic fragments (Johnsson *et al.,* 1988; Itiowe *et al.,* 2021); neither of which are seen in the Ghaggar-Hakra Formation. Considering the observations and interpretations above we argue for multi-cycle quartzose arenites.

Knowledge of the palaeo-topography and palaeo-climate is key to understanding the number of cycles these quartzose arenites have been through and the relative contribution of weathering to the detrital composition. The warm but dry sub-tropical palaeoclimate is highly unlikely to generate first cycle quartzose arenites (Suttner *et al*., 1981), further supporting that the Ghaggar-Harka sediments are at least second cycle. The first cycle of quartzose arenites of the WIRS originate from the Aravalli Range in the Jodhpur Group and are then reworked at least once in the Mesozoic to be redeposited as the Ghaggar-Hakra Formation. Given that the sedimentary grains from the Jodhpur Group display few quartz overgrowths (Kumar *et al*., 2011) and microbial mat growth (Samanta *et al.,* 2011) overgrowths in the Ghaggar-Hakra sediments are unlikely. Similar conclusions have been reached for the Bhuj Formation based on zircon geochronology (Anderson *et al.,* 2018; Chaudhuri *et al*., 2020b).

Fluvial transport pathways

During Early Cretaceous times, clastic deposition across the north-western Indian Plate was dominated by fluvial systems that carried sediment to coastal plains and deltas forming along the northern edge of the Indo-Tethyan Ocean (Beaumont *et al*., 2019). The depth to top basement map for north-west India of Kothari *et al*. (2015) is here used to define a detailed structural framework that depicts the distribution of the Early Cretaceous rift systems which in turn define the depositional systems. The leading edge of the Indian Plate comprised much of present-day Pakistan where the Lower Cretaceous sediments were deposited in coastal embayments, deltas, and shorefaces (Ahmad *et al*., 2012; Smewing *et al*., 2002). Madagascar had not yet separated from India (Bastia *et al*., 2010; Chatterjee *et al*., 2013) so the present-day Gulf of Khambat and Mumbai Offshore Basin were represented by an incipient rift basin, orientated orthogonally to the Cambay Basin, that extended around the Saurashtra Arch coastline (Beaumont *et al*., 2019). Measured palaeoflow directions indicated by the sediments of the Ghaggar-Hakra Formation are to the south-west (Sisodia & Singh, 2000; Bladon *et al*., 2015; Beaumont *et al*., 2019) and into the Barmer Basin, reflecting their deposition on a relay ramp (the Saraswati Terrace) that fed alluvial fans on the basin edge. Flow was probably directed southwards from the fans by fluvial systems developed along the axis of the rift, towards the Cambay Basin (Figure 14). Therefore, it is likely that alluvial and fluvial systems draining from the southern Aravalli Mountains fed sediment into the Barmer and Cambay basins and possibly on into a poorly known, Early Cretaceous, rift basin beneath the present-day Gulf of Khambhat and Mumbai Offshore Basin. In this interpretation, sediments were transported over some 600 km along the axial-distance of the Barmer and Cambay rifts and potentially a further 200 km along a rift basin beneath the Gulf of Khambhat and Mumbai Offshore Basin, after they had been transported for almost 400 km across alluvial plains from the Aravalli Range.

Whilst this view of provenance to the northeast and east is broadly aligned with that of Chaudhuri *et al*. (2020a, 2020b), it is probable that the source area for the Kachchh Basin is the Nagar Parkar Ridge to the north (Ahmad & Bhat, 2006; Ramakrishnan & Vaidyanadhan, 2008; Valdiya, 2015) and the western high flanking the Cambay Basin (see Beaumont et al., 2019). First cycle derivation of the Kachchh Basin sandstones from the Aravalli Range to the east is unlikely because of the development of the intervening Barmer and Cambay rift basins (Figure 14) which must have been barriers to fluvial transport. Once within these rifts, Lower Cretaceous sediments would have been retained within the rifts and transported axially. More likely, as Chaudhuri *et al*. (2021) speculate, is the presence of hidden orogenic rocks in northwest India which, although not cropping out present-day, served as the main source of sediment for the Mesozoic strata of Kachchh Basin.

Early Cretaceous rivers draining the Devikot High and the northern Aravalli Range probably supplied sediment for the strata of the Lower Goru and Sembar formations of the LMIBs across the Punjab Platform. They may have been fed by tributaries draining the Devikot Ridge (Beaumont *et al.*, 2019), which potentially accounts for their more feldspar-rich mineralogy. Here, the palaeogeographical reconstruction of Figure 14 suggests a much more complex drainage system than has previously been envisaged for the northern leading edge of the Indian Plate. Upland deposits had very low preservation potential which, compounded with later uplift and widespread erosion preceding the Deccan volcanism, resulted in the disparate preservation of fluvial Lower Cretaceous sediments. Most of the Lower Cretaceous sediments preserved in the WIRS are remnants of a syn-rift continental succession (Biswas, 1999). By contrast, the coastal plain and deltaic deposits of the Sembar-Lower Goru succession of the LMIB were much more regionally extensive at deposition when compared to the WIRS and accumulated along the Indo-Tethyan leading edge in coastal plain, deltaic, and shallow marine shoreface settings.

Conclusions

Lower Cretaceous (Aptian-Albian) sandstones of the Ghaggar-Hakra Formation are quartzose arenites with a complex diagenetic history. Reconstruction of the original depositional mineralogy indicates that diagenesis alone cannot account for the quartzose arenite composition, despite Early Cretaceous soil formation and at least two periods of subsequent telogenetic modification. The absence of intense tropical weathering in northwest India during the Early Cretaceous Period supports this interpretation.

Palaeogeographical reconstructions indicate the Ghaggar-Hakra Formation quartzose arenites were most probably derived from the recycling of Late Neoproterozoic to Lower Cambrian sandstones, principally the Jodhpur Group, which were exposed across large areas of northwest India. The sandstones of the Jodhpur Group are compositionally quartzose arenites but were derived from a provenance comprising the metamorphosed pelites of Delhi Supergroup, banded Precambrian gneiss and the Erinpura granite basement in the Aravalli Mountains. Petrographical and heavy-mineral analysis of the Ghaggar-Hakra sandstones indicates that there are no stratigraphical trends in detrital mineralogy.

The failed rifts of the Barmer and Cambay basins form a natural transport barrier that precluded the transport of detritus from the Aravalli Mountain Range across these deep rifts into the more westerly rift basins of the Kachchh and South Indus basins. Sediment detritus delivered to the Barmer and Cambay basins remained within this rift system where axial transport delivered it generally southwards into the Mumbai Offshore Basin. Variations in detrital mineralogy across the WIRS and LMIB is the result of fluvial transport systems sourced from multiple highs and controlled by the rift palaeogeographies.

Data Availability Statement:

The data that supports the findings of this study are available in the supplementary material of this article

References

Afzal, J., Williams, M. and Aldridge, R.J. 2009. Revised stratigraphy of the lower Cenozoic succession of the Greater Indus Basin in Pakistan. Journal of Micropalaeontology, 28, 7-23

Ahmad, A.H.M. and Akhtar, K. 1990. Clastic environments and facies of the Lower Cretaceous Narmada Basin, India. Cretaceous Research, 11, 175-190.

Ahmad, A.H.M and Bhat, G.M. 2006 Petrofacies, provenance and diagenesis of the Dhosa sandstone member (Chari Formation) at Ler, Kachchh sub-basin, Western India. Journal of Asian Earth Sciences 27, 857–72, https://doi.org/10.1016/j.jseaes.2005.08.005.

Ahmad, A.H.M., Alam M. and Khan, H.A. 2000 Texture and Petrofacies analysis of Sandstones of the Lathi Formation (early Jurassic), Western Rajasthan. Indian Jl Petroleum Geology, 9, 59-70.

Ahmad, N. and Chaudhry, S. 2002. Kadanwari Gas Field, Pakistan: a disappointment turns into attractive development opportunity. Petroleum Geoscience, 8, 307-316.

Ahmad, N., Fink, P., Sturrock, S., Mahmood, T., and Ibrahim, M., 2012. Sequence Stratigraphy as Predictive Tool in Lower Goru Fairway, Lower and Middle Indus Platform, Pakistan. AAPG Search and Discovery Article #10404.

Akhtar, K., and Ahmad, A.H.M., 1991. Single cycle cratonic quartzarenites produced by tropic weathering: the Nimar sandstones (Lower Cretaceous), Narmada Basin, India. Sedimentary Geology, 71, 23-32.

Akhtar, K., Khan, A.Z. and Ahmad, A.H.M., 1996. Anomalous quartzarenites of a Lower Cretaceous rift basin: Wadhwan Formation of Western India. Bulletin of the Geological Society of Malaysian, 39, 81-90.

Affolter, M.D. and Ingersol, R.V. 2019. Quantitative analysis of volcanic lithic fragments. Journal of Sedimentary Research, 89, 479–486.

Alam, M.M., Ahmad, A.H.M. and Khan, M.H.A. 2000. Diagenetic features of Lower Jurassic Lathi Sandstones, Jaisalmer Basin, Western Rajasthan. Jl Geol. Soc. India, 56, 415-424.

Ali, J.R. and Aitchison, J.C. 2014. Greater India's northern margin prior to its collision with Asia. Basin Research, 26, 73-84.

Anand, R.R., 2002. Weathering history, landscape evolution and implications for exploration: In: Butt, C.R.M., Cornelius, M., Scott, K.M. and Robertson, I.D.M. (Eds.), Regolith Expression of Australian Ore Systems, CRC, LEME (2011), 15-45.

Anderson, T., Elburg, M.A., van Niekerk, H.S. and Ueckermann, H. 2018. Successive sedimentary recycling regimes in southwestern Gondwana: Evidence from detrital zircons in Neoproterozoic to Cambrian sedimentary rocks in southern Africa. Earth-Science Reviews, 181, 43-60.

Andò, S., & Garzanti, E. (2014). Raman spectroscopy in heavy-mineral studies. Geological Society, London, Special Publications, 386(1), 395-412.

Aquil, M., 1982. Petrography and Palaeocurrents of the Himatnagar Sandstone (Cretaceous) in the Vicinity of Himatnagar Town, Sabarkantha District, Gujarat State. MSc Publication Aligarh Muslim University.

Augustsson, C., 2021. Influencing Factors on Petrography Interpretations in Provenance Research—A Case-Study Review. Geosciences, 11, 205. https://doi.org/10.3390/geosciences11050205

Baig, M.O., Harris, N.B., Ahmed, H. and Baig, M.O.A. 2016. Controls on reservoir diagenesis in the Lower Goru Sandstone Formation, Lower Indus Basin, Pakistan. Jl. Pet. Geol., 39, 29-48.

Balakrishnan, T.S., Unnikrishnan, P. and Murty, A.V.S. 2009. The Tectonic Map of India and Contiguous Areas. Journal of the Geological Society of India, 74, 158-170.

Bastia, R., Reeves, C., Rao, D.P., D'Silva, K. and Rahakrishna, M. 2010. Palaeogeographic reconstruction of East Gondwana and evolution of the Indian continental margin. DCS-DST news August, 2-8.

Basu, A., Schieber, J., Patranabis-Dev, S. and Dhang, P.C. 2013. Recycled detrital quartz grains are sedimentary rock fragments indicating unconformities: Examples from the Chhattisgarh Supergroup, Bastar Craton, India. Journal of Sedimentary Research, 83, 368-376.

Bata, T. 2016. Evidence of widespread Cretaceous deep weathering and its consequences: a review. Earth Science Res., 5, 69-84.

Beaumont, H., Clarke, S.M., Burley, S.D., Talyor, A., and Mohapatra, P. (2019) Sedimentology and the facies architecture of the Ghaggar-Hakra Formation, India: Implications for early Cretaceous deposition on the north-western Indian Plate margin. Depositional record, 5(1) 53-83.

Berger, A., Gier, S., and Krois, P., 2009. Porosity-preserving chlorite cements in shallow-marine volcaniclastic sandstones: Evidence from Cretaceous sandstones of the Sawan gas field, Pakistan. American Association of Petroleum Geologists 93, 595-615.

Bhatt, N.Y., Solanki, P.M., Prakash, N., Das, N., 2016. Depositional environment of Himmantnagar Sandstone (Lower/Middle Cretaceous): a perspective, The Palaeobotanist, 56, 67-84.

Bhattacharya, A.R., Singh, S.P., 2013. Proterozoic crustal-scale shearing in the Bundelkhand massif with special reference to quartz reefs. Journal of the Geological Society of India, 82, 474-484.

Bhushan, S.K., 1985. Malani volcanism in western Rajasthan. Indian Journal of Earth Sciences, 12, 58-71.

Bhushan, S.K., 1985. Malani Volcanism in western Rajasthan. Indian Journal of Earth Sciences, 12(1), 58-71.

Biju-Sekhar, S., Yokoyama, K., Pandit, M.K., Okudaira, T., Yoshida, M. and Santosh, M. 2003. Late Paleoproterozoic magmatism in Delhi Fold Belt, NW India and its implication: evidence from EPMA chemical ages of zircons. Journal of Asian Earth Sciences, 22, 189-207.

Biswas, S.K., 1987. Regional tectonic framework, structure and evolution of the western marginal basins of India. Tectonophysics 135, 307-327.

Biswas, S.K., 1999. A review on the evolution of rift basins in India during Gondwana with special reference to western Inbosedian basins and their hydrocarbon prospects. Proceedings of the National Indian Science Academy 65, 261-283.

Biswas, S.K., 2005. A review of structure and tectonics of Kutch Basin, western India, with special reference to earthquakes. Current Science, 88(10), 1592-1600.

Bjorkum, P.A., and Gjelsvik, N., 1988. An isochemical model for formation of authigenic kaolinite, K-feldspar and illite in sediments. Journal of Sedimentary Petrology 58(3), 506-511.

Bladon, A.J., Burley, S.D., Clarke, S.M., and Beaumont, H., 2015. Geology and regional significance of the Barmer Basin, northwest India. Basin Research, 27, 636-655.

Blatt H. (1982) Sedimentary petrology, Arizona, W.H. Freeman and Company.

Bose P.K., Shome S., Bardhan S and Ghosh G. (1986) Facies mosaic in the Ghuneri Member (Jurassic) of the Bhuj Formation, western Kutch, India, Sedimentary Geology, 46, 293 – 309.

Casshyap, S.M., and Aslam, M., 1992. Deltaic and shoreline sedimentation in Saurashtra Basin, western India: An example of infilling in an early Cretaceous failed rift. Journal of Sedimentary Petrology, 62, 972-991.

Chatterjee, S., Goswami A., Scotese C.R., 2013. The longest voyage: Tectonic, magmatic and paleoclimate evolution of the Indian plate during its northward flight from Gondwana to Asia. Gondwana Research, 23(1), 238-267.

Chaudhuri A, Banerjee, S. and Le Pera, E. 2018. Petrography of Middle Jurassic to Early Cretaceous sandstones in the Kutch Basin, western India: Implications on provenance and basin evolution. Journal of Palaeogeography, 7(2) https://doi.org/10.1186/s42501-018-0002-6

Chaudhuri A, Banerjee S and Chauhan G. 2020a. Compositional evolution of siliciclastic sediments recording the tectonic stability of a pericratonic rift: Mesozoic Kutch Basin, western India. Marine and Petroleum Geology, 111, 476–95, https://doi.org/10.1016/j.marpetgeo.2019.08.026.

Chaudhuri, A., Banerjee, S., Das, K. and Le Pera, E. 2021. Evidence of lost orogenies in the Mesozoic sedimentary record of the Kutch Basin, western India. IAS 35th Annual Meeting Abstracts (Prague 2021), Contribution ID 264.

Chaudhuri, A., Das, K., Banerjee, S., and Fitzsimons, I.C.W., 2020b. Detrital zircon and monazite track the source of Mesozoic sediments in Kutch to rocks of Late Neoproterozoic and Early Palaeozoic orogenies in northern India. Gondwana Research, 80, 188-201.

Chaudhuri, A., Chatterjee, A., Banerjee, S. and Ray, J.S. 2020c. Tracing multiple sources of sediments using trace element and Nd isotope geochemistry: provenance of the Mesozoic succession in the Kutch Basin, western India Geological Magazine https://doi.org/10.1017/S0016756820000539

Chopparapu, C. and Rajanikanth, A. 2018. Mesozoic woods from India: Nomenclature review and palaeoclimatic implications. Palaeoworld, 2, 211-225.

Collier, J.S., Sansom, V., Ishizuka, O., Taylor, R.N., Minshull, T.A., and Whitmarsh, R.B., 2008. Age of Seychelles-India break-up. Earth and Planetary Sciences Letters, 272, 264-277.

Compton, P.M., 2009. The geology of the Barmer Basin, Rajasthan, India and the origins of its major oil reservoir, the Fatehgarh Formation. Petroleum Geoscience, 15, 117-130.

Cox, K.G., 1989. The role of mantle plumes in the development of continental drainage patterns. Nature, 88, 873-877.

Davies, J. K., Meert, J.G. and Pandit, M.K. 2014. Paleomagnetic analysis of the Marwar Supergroup, Rajasthan, India and proposed interbasinal correlations. Journal of Asian Earth Sciences, http://dx.doi.org/10.1016/j.jseaes.2013.09.027

Desai A.G. and Desai S.J. (1989) Himatnagar Sandstones of north Gujarat their depositional environment and tectonic framework, Ph.D. Thesis, Maharaja Sayajirao University of Baroda.

Dickinson, W.R., 1985. Interpreting provenance relations from detrital modes of sandstone, NATO ASI Series 148, 333-361.

Dickinson, W.R., and Suczek, C.A., 1979. Plate tectonics and sandstone compositions. American Association of Petroleum Geology Bulletin 63(12), 2164-2182.

Dickinson W.R., 1970. Interpreting detrital modes of graywacke and arkose. Journal of Sedimentary Research, 40(2), 695-707.

Dickinson, W.R., Beard L.S., Robert-Brakenridge G., Erjavec J.L., Ferguson R.C., Inman K.F., Knepp R.A., Lindberg F.A. and Ryberg P.T. 1983. Provenance of North American Phanerozoic sandstones in relation to tectonic setting, Geological Society of American Bulletin, 94, 222 – 235.

Diko, M.L. 2013. From source to basin of deposition: influence of transportation and diagenesis on geophagic properties of soil, Transactions of the Royal Society of South Africa, 68:3, 183-191, DOI: 10.1080/0035919X.2013.847128.

Dolson J., Burley S.D., Sunder, V.R., Kothari, V., Naidu B., Whiteley, N.P., … Ananthakrishnan, B., 2015. The discovery of the Barmer Basin, Rajasthan, India and its petroleum geology. American Association of Petroleum Geology Bulletin, 99, 433-465.

Driese, S.G., Simpson, E.L. & Eriksson, K.A. 1995. Redoximorphic paleosols in alluvial and lacustrine deposits, 1.8 Ga Lochness Formation, Mount Isa, Australia: pedogenic processes and implications for paleoclimate. Journal of Sedimentary Research. 65, 675–689.

Dunkl, I., et al. (2020). Comparability of heavy mineral data–The first interlaboratory round robin test. Earth-Science Reviews, 211, 103-210.

Dutta, P.K., 1992. Chapter 4 Climate Influence on Diagenesis of Fluvial Sandstones. Developments in Sedimentology, 42, 191-252

Ehrenberg, S.N. 1989. Assessing the Relative Importance of Compaction Processes and Cementation to Reduction of Porosity in Sandstones: Discussion; Compaction and Porosity Evolution of Pliocene Sandstones, Ventura Basin, California: Discussion 1 The American Association of Petroleum Geologists Bulletin, 73(10), 1274-1276

Ehrenberg, S.N. 1995. Measuring sandstone compaction from modal analyses of thin sections: how to do it and what the results mean. Journal of Sedimentary Research, A65(2), 369-379

Garzanti E. and Vezzoli G. (2003) A classification of metamorphic grains in sands based on their composition and grade, Journal of Sedimentary Research, 73, 830 – 837

Garzanti, E. 2016. From static to dynamic provenance analysis—Sedimentary petrology upgraded. Sedimentary Geology, 336, 3–13.

Garzanti, E. 2019. Petrographic classification of sand and sandstone. Earth Science Reviews, 192, 545-563.

George, B.G. and Ray, J.S. 2017. Provenance of sediments in the Marwar Supergroup, Rajasthan, India: Implications for basin evolution and Neoproterozoic global events. Journal of Asian Earth Sciences, 147, 254–270.

Gombos, A.M., Powell, W.G., and Norton, I.O., 1995. The tectonic evolution of western India and its impact on hydrocarbon occurrences: an overview. Sedimentary Geology, 96, 119-129.

Goodwin, A.M., 1991. Precambrian Geology the dynamic evolution of the continental crust, London, UK, Academic Press Limited.

Goswami, A. 2011. Predicting the geographic distribution of ancient soils with special reference to the Cretaceous. Ph.D. Thesis, University of Texas, Arlington, Texas.

Haile, B.G., Line, L.H., Klausen, T.G., Olaussen, S., Eide, C.H., Jahren, J. and Hellevang, H. 2021. Quartz overgrowth textures and fluid inclusion thermometry evidence for basin-scale sedimentary recycling: An example from the Mesozoic Barents Sea Basin. Basin Research, 33, 1697-1710.

Harris, N.B. 1989. Diagenetic quartzarenite and destruction of secondary porosity: an example from the Middle Jurassic Brent sandstones of northwest Europe. Geology, 17, 361-364.

Helmold, K.P. 1985. Provenance of feldspathic sandstones—The effect of diagenesis on provenance interpretations: A review. In Provenance of Arenites; Zuffa, G.G., Ed.; Springer: Dordrecht, The Netherlands, pp. 139–163.

Henry, D.J., and Guidotti, C.V., 1985. Tourmaline as a petrogenetic indicator mineral: an example from the staurolite-grade metapelites of NW Maine. American Mineralogist, 70, 1-15.

Heron, A.M. 1953. The geology of central Rajaputana. Memoirs of the Geological Survey of India, 79, 389.

Housenecht, D.W. 1987. Assessing the relative importance of compaction processes and cementation to reduction of porosity in sandstones. The American Association of Petroleum Geologists Bulletin, 71(6), 633-642.

Hubert, J.F. (1962). A zircon-tourmaline-rutile maturity index and the interdependence of the composition of heavy mineral assemblages with the gross composition and texture of sandstones. Journal of Sedimentary Research, *32*(3), 440-450.

Ismail, S., Moshin, S.I., Shah, S.K.A. and Ismail, S. 2018. Clay Mineralogy and Petrography of Basal Sand Reservoir of Badin Block, Southern Indus Basin, Pakistan: Implications for Diagenesis and Reservoir Damage Potential Assessment. International Journal of Economic and Environmental Geology, 9 49-57.

Itiowe, K., Odigi, M.I., Kurah, B.K. and Kpegeol, B. 2021. Petrography and Provenance of Eze-Aku

Sandstones in Afikpo Basin, Southeastern Benue Trough. Asian Journal of Geological Research, 4, 54-64.

Jennings D.S., Driese, S.G. and Dworkin, S.I. 2015. Comparison of modern and ancient barite-bearing acid-sulphate soils using micromorphology, geochemistry and field relationships. Sedimentology, 62, 1078–1099.

Johnsson, M.J., Stallard, R.F. and Meade, R.H. 1988. First-cycle quartz arenites in the Orinoco River Basin, Venezuela and Colombia. Journal of Geology 96, 263-277.

Kothari, V., Naidu, B., Sunder, V.R., Dolson, J., Burley, S.D., Whiteley, N.P., … Ananthakrishnan, B., 2015. Discovery and petroleum system of Barmer Basin, India. (abs.): AAPG Search and discovery article #110202.

Kotowski, J., Nejbert, K., and Olszewska-Nejbert, D., 2020. Tourmalines as a Tool in Provenance Studies of Terrigenous Material in Extra-Carpathian Albian (Uppermost Lower Cretaceous) Sands of Miechów Synclinorium, Southern Poland. Minerals. 10; doi:10.3390/min10100917

Krishna, J. 1987. An overview of the Mesozoic stratigraphy of Kachchh and Jaisalmer Basin. Journal of Palaeontology Society India. 32, 136–149.

Kumar, S., Pandey, S.K. and Ahmad, A. 2011. Occurrence of giant nodules in the Jodhpur Sandstone, Sursagar area, Jodhpur, Rajasthan. Current Science, 100, 1294-1296.

Kundal, P., and Sanganwar, B.N., 1998. Stratigraphy and Palichnology of Nimar Sandstone, Bagh Beds of Jobat Area, Jhabua District, Madhya Pradesh. Journal Geological Society of India, 51, 619-634.

Mahashwari A. Sial A.N. and Mathur S.C. (2000) Carbon isotope fluctuations through the Neoproterozoic-lower Cambrian Birmania Basin, Rajasthan, India. Carbonates and Evaporites, 17, 53 – 59.

Mahashwari A., Sial A.N. and Mathur S.C. (2007) Carbon-13 stratigraphy of the Birmania Basin, Rajasthan, India: implications for the Vendian – Cambrian transition, In: Vickers-rich, P. & Komarower,

P. (eds) The Rise and Fall of the Ediacaran Biota, Geological Society, London, Special Publications, 286, 439–441.

Mandal, A., Koner, A., Sarkar, S., Tawfik, H.A., Chakraborty, N., Bhakta, S., Bose, P.K. 2016. Physico-chemical tuning of palaeogeographic shifts: Bhuj formation, Kutch, India. Marine and Petroleum Geology, 78, 474–492. https://doi.org/10.1016/j.marpetgeo.2016.10.003.

Mange, M.A., and Maurer, F.W., 1992. Heavy minerals in colour. No location given: Chapman and Hall. 11-17.

Marks, K.M. and Tikku, A.A. 2001. Cretaceous reconstructions of East Antarctica, Africa and Madagascar. Earth and Planetary Science Letters, 186, 479-495.

McBride, E.F. 1985. Diagenetic processes that affect provenance determinations in sandstone. In Provenance of Arenites; Zuffa, G.G., Ed.; Springer: Dordrecht, The Netherlands, pp. 95–115.

McKenzie, N.R., Hughes, N.C., Myrow, P.M., Xiao, S., Sharma, M., 2011. Correlation of Precambrian-Cambrian sedimentary successions across northern India and the utility of isotopic signatures of Himalayan lithotectonic zones. Earth and Planetary Science Letters, 312, 471–483.

McKenzie, N.R., Hughes, N.C., Myrow, P.M., Banerjee, D.M., Deb, M., Planavsky, N.J., 2013. New age constraints for the Proterozoic Aravalli–Delhi successions of India and their implications. Precambrian Research, 238, 120–128.

Millett, J.W., Jerram, D.A., Planke, S., Mund, B.K., Konar, S., Sharda, R., Maharjan, D. and Patankar, T. 2021. Volcanic facies architecture of early bimodal volcanism of the NW Deccan Traps: Volcanic reservoirs of the Raageshwari Deep Gas Field, Barmer Basin, India. Basin Research, https://doi.org/10.1111/bre.12605

Mohan, M., 1995. Cambay Basin – A promise of oil and gas potential. Journal of the Palaeontological Society of India. 40, 41-47.

Moral Cardona, J.P., Gutierrez Mas, A. Bellon, A. S., Lopez-Aguayo, F. and Caballero, M.A. 1997. Provenance of multicycle quartz arenites of Pliocene age at Arcos, southwestern Spain. Sedimentary Geololgy, 112, 251-261.

Morton, A. C. (1985). Heavy minerals in provenance studies. In Provenance of arenites, G.G. Zuffa (ed.), (249-277). Springer, Dordrecht.

Morton, A. C. (1986). Dissolution of apatite in North Sea Jurassic sandstones: implications for the generation of secondary porosity. Clay minerals, 21(4), 711-733.

Morton, A. and Hurst, A. 1995. Correlation of sandstones using heavy minerals: an example from the Statfjord Formation of the Snorre Field, northern North Sea. Geological Society, London, Special Publications, 89, 3-22

Morton A.C., and Chenery, S. 2009. Detrital rutile geochemistry and thermometry as guides to provenance of Jurassic-Paleocene sandstones of the Norwegian Sea. Journal of Sedimentary Research, 79(7), 540-553.

Mude, S.N., Jagtap, S.A., Kundal, P., Sarkar P.K., and Kundal M.P., 20120. Paleoenvironmental significance of ichnofossils from the Mesozoic Jaisalmer Basin, Rajasthan, north western India. Proceedings of the International Academy of Ecology and Environmental Sciences 2(3), 150-167

Mukherjee, M.K. 1983. Petroleum prospects of Cretaceous sediments of the Cambay Basin, Gujarat, India. Journal of Petroleum Geology 5, 275-286.

Naidu, B.N.S., Burley, S. D., Dolson, J., Farrimond, P., Sunder, V.R., Kothari, V. and Mohapatra, P. 2017. Hydrocarbon generation and migration modelling in the Barmer Basin of western Rajasthan, India: lessons for exploration in rift basins with late stage inversion, uplift and tilting. In: M. A. Abu-Ali, I. Moretti, and H. M. Bolas (eds) Petroleum Systems Analysis, American Association of Petroleum Geologists Memoir 114, 69-90.

Najman, Y., Burley, S.D., Copley, A., Kelly, M.J., Pander, K., and Mishra, P. 2018. The Oligo-Miocene unconformity of the Himalayan and NW Indian Intraplate basins: a record of tectonics or mantle dynamics? Tectonics, 37, 3970-3985.

NDR database, 2021. National Data Repository, Directorate General of Hydrocarbon (DGH), Ministry of Petroleum and Natural Gas, Government of India. Online: https://www.ndrdgh.gov.in/NDR/ Data accessed: 28/12/2021

Nasseer T.M., Asim S., Ahmad M.N., Hussain F., and Qureshi S.N., 2014. Application of Seismic Attributes for Delineation of Channel Geometries and Analysis of Various Aspects in Terms of Lithological and Structural Perspectives of Lower Goru Formation, Pakistan. International journal of geosciences 5, 1490-1502.

Pandey, D.K., Fursich, F.T., and Sha, J-G., 2009. Interbasinal marker intervals – A case study from the Jurassic basins of Kachchh and Jaisalmer, western India. Science in China Press, 52, 1924-1931.

Pandey, D.K., Choudhary, S., Bahadur, T., Swami, N., Poonia, D. and Sha, J-G., 2012. A review of the Lower – lowermost Upper Jurassic facies and stratigraphy of the Jaisalmer Basin, western Rajasthan, Volumina Jurassica, 10, 61-82.

Phethean, J.J.J., Kalnins, L.M., van Hunen, J., Biffi, P. G., Davies, R.J. and McCaffrey, K. J.W. 2016. Madagascar's escape from Africa: A high-resolution plate reconstruction for the Western Somali Basin and implications for supercontinent dispersal. Geochemistry, Geophysics, Geosystems, 17, 5036–5055. doi:10.1002/2016GC006624

Powell, C.McA. and Conaghan, P.J. 1973. Plate tectonics and the Himalayas. Earth and Planetary Science Letters, 20, 1-12

Racey, A., Fisher, J., Bailey, H., and Kumar-Roy, S., 2016. The value of fieldwork in making connections between onshore outcrops and offshore models: an example from India. Geological Society of London, Special Publications, 436, 21-53.

Rahman, M.M., Hasan, M.F., Hasan, A.S.M., Alam, M.S., Biswas, P.K. and Zaman, M.N. 2021. Chemical weathering, provenance, and tectonic setting inferred from recently deposited sediments of Dharla River, Bangladesh. Journal of Sedimentary Environments, https://doi.org/10.1007/s43217-020-00046-z.

Rajak, P.K., Chaudhuri, A., Prabhakar, N. and Banerjee, S. 2022. Tracking sources and paleotectonic settings of Mesozoic sandstones in interlinked rift basins of western India: An integrated approach using petrography and heavy mineral chemistry. Journal of Palaeogeography, 11, 173-193.

Rao, J.M., Rao, G.V.S.P., Widdowson, M., Kelley, S.P., 2005. Evolution of Proterozoic mafic dyke swarms of the Bundelkhand Granite Massif, Central India. Current Science, 88, 502-506.

Ramakrishnan M and Vaidyanadhan R (2008) Geology of India, pp. 261–333. Bangalore: Geological Society of India.

Roy, A.B., and Jokhar, S.R., 2002. Geology of Rajasthan (Northwest India) Precambrian to recent, Pawan Kumar. Scientific Publishers, India. Jodhpur, India.

Salama, W., Anand, R. (2017) Reconstructing the pre-Quaternary landscape in Agnew-Lawlers area, Western Australia with emphasis on the Permo-Carboniferous glaciation and post-glacial weathering. International Journal of Earth Sciences, 106, 311-339.

Samanta, P., Mukhopadhyay, S., Mondal, A. and Sarkar, S. 2011. Microbial mat structures in profile: The Neoproterozoic Sonia Sandstone, Rajasthan, India. Journal of Asian Earth Sciences, 40, pp 524-549.

Schumm, S.A., 1981. Evolution and response of the Fluvial System, sedimentological implications. The Society of Economic Palaeontologists and Mineralogists (SEPM), Special Publications, 31, 19-29.

Scotese, C.R. 2011. The PALEOMAP Project paleoatlas for ArcGIS, volume 2, Cretaceous paleogeographic and plate tectonic reconstructions. PALEOMAP Project, Arlington, Texas.

Scotese, C.R., Illich, H., Zumberge, J. and Brown, S. 2007. The GANDOLPH Project: One-year report: Paleogeographic and palaeoclimate controls on hydrocarbon source rock deposition, A report on the methods employed, the results of the paleoclimate simulations (FOAM) and oil/source rock compilation for the late Cretaceous (Cenomanian/Turonian; 93.5 Ma), late Jurassic (Kimmeridgian/Tithonioan; 151 Ma), Early Permian (Sakmarin/Artinskian; 248 Ma) and late Devonian (Frasnian/Femennian; 372 Ma), Conclusions at the end of year one. GeoMark Research LTD, Houston, Texas.

Sharma, A., Sahoo, S., Rao, N.V.C., Belyatsky, B., Dhote, P. and Lehmann, B. 2021. Petrology and Nd–Sr isotopic composition of alkaline lamprophyres from the Early to Late Cretaceous Mundwara Alkaline Complex, NW India: evidence of crystal fractionation, accumulation and corrosion in a complex magma chamber plumbing system. In: Krmíček, L. and Chalapathi Rao, N. V. (eds) Lamprophyres, Lamproites and Related Rocks: Tracers to Supercontinent Cycles and Metallogenesis. Geological Society, London, Special Publications, 513, https://doi.org/10.1144/SP513-2020-175.

Sharma, K.K., 2000. Evolution of Archean Palaeoproterozoic crust of the Bundelkhand Craton, Northern Indian Shield. Research Highlights in Earth System Congress, 95-105.

Sheth, H.C., 2007. Plume-related regional pre-volcanic uplift in the Deccan Traps: Absence of evidence, evidence of absence. The Geological Society of America Special Paper, 430, 785-813.

Singh, N.P. 2006. Mesozoic Lithostratigraphy of the Jaisalmer Basin, Rajasthan. Journal of the Palaeontological Society of India 52, 1-25.

Singh, S.P. 1988. Sedimentation patterns of the Proterozoic Delhi Supergroup, northeastern Rajasthan, India, and their tectonic implications. Sedimentary Geology, 58, 79-94.

Singh, S.P., Divedi, S.B., 2015. High grade metamorphism in the Bundelkhand massif and its implications on Mesoarchean crustal evolution in central India. Journal of Earth System Science, 124, 197-211.

Sisodia, M.S., and Singh, U.K., 2000. Depositional environment and hydrocarbon prospects of the Barmer Basin, Rajasthan, India. North American Free Trade Association 9, 309–326.

Smewing, J.D., Warburton, J., Daley, T., Copestake, P. and Ul-haq, N. 2002. Sequence stratigraphy of the southern Kirthar Fold Belt and Middle Indus Basin, Pakistan: In: Clift, P.D., Gaedicke, D., Craig, J., (eds). The tectonics and climatic evolution of the Arabian Sea Regions; geological Society, London, Special Publications, 195, 273-299.

Srivastava D.C., Rao, P.V. and Hardas M.G. (1980) Depositional environment of Mesozoic sediments of Saurashtra revealed by textural parameters, Journal of the Palaeontological Society of India, 23, 136 – 139

Suttner, L.J., Basu, A. and Mack, G.H. 1981. Climate and the origin of quartz arenites. Journal of Sedimentary Petrology, 51(4) 1235-1246

Tabaei, M., and Singh, R.Y., 2002. Paleoenvironment and paleoecoligical significance of microforaminiferal linings in the Akli Lignite, Barmer Basin, Rajasthan, India. Iranian International Journal of Science, 3, 263-277.

Torsvik, T.H., Tucker, R.D., Ashwal, L.D., Carter, L.M., Jamtveit, B., Vidyadharan, T. and Venkataramana, P. 2000. Late Cretaceous India-Madagascar fit and timing of break-up and related magmatism. Terra Nova, 12, 220-225.

Tripath, S.K.M., Kumar, M. and Srivastava, D., 2009. Palynology of Lower Palaeogene (Thanetian-Ypresian) costal deposits from the Barmer Basin (Akli Formation, Western Rajasthan, India): Palaeoenvironmental and palaeoclimatic implications. Geological Acta, 7, 147-160.

Tucker, M.E., 2001. Sedimentary Petrology Analysis, (3rd Ed.), Oxford, UK, Blackwell Science

Vijayan, A., Sheth, H. and Sharma, K.K. 2016. Tectonic significance of dykes in the Sarnu-Dandali alkaline complex, Rajasthan, northwestern Deccan Traps. Geoscience Frontiers, 7, 783-791.

Vine, J.D., and Tourtelot, E.B., 1970. Preliminary geochemical and petrographical analysis of lower Eocene fluvial sandstones in the Rocky Mountain Region, Book/Publication Symposium on Wyoming Sandstones: Their Economic Importance—Past, Present & Future; 22nd Annual Field Conference Guidebook.

Von Eynatten, H. and Dunkl, I. 2012. Assessing the sediment factory: The role of single grain analysis. Earth-Science Reviews, 115, 97–120. https://doi.org/10.1016/j.earscirev.2012.08.001

Wandrey, C.J., Law, B.E. and Shah, H.A., 2004. Sembar Goru/Ghazij composite total petroleum system, Indus and Sulaiman-Kirthar geologic provinces Pakistan and India. United States Geological Survey Bulletin 2208-C.

Widdowson, M. 1997. Tertiary palaeosurfaces of the SW Deccan, Western India: Implication for passive margin uplift. In: Palaeosurfaces: Recognition, Reconstruction and Palaeoenvironmental Interpretation (ed.) Widdowson, M., Geological Society Special Publications, 120, 221–248

Wilkinson, M. and Haszeldine, R.S. 1996. Aluminium loss during sandstone diagenesis. J. Geol. Soc. Lond., 153, 657–660.

Worden, R.H.; Burley, S.D. 2003. Sandstone diagenesis: The evolution of sand to stone. In Sandstone Diagenesis: Recent and Ancient; Burley, S.D. and Worden, R.H., (Eds).; Blackwell Publishing, pp. 3–44.

Zadan, K. and Arbab, K.A. 2015. A review on lithostratigraphy and biostratigraphy of Jaisalmer Basin, Western Rajasthan, India. International Research Journal of Earth Science, 3, 37-45